GEOPHYSICAL TRANSACTIONS 2000
Vol. 43. No. 1. p. 64

Erratum

Emő MÁRTON and Péter MÁRTON 1999. Tectonic aspects of a palaeomagnetic study on the Neogene of the Mecsek Mountains. Geophysical Transactions **42,** 3 – 4, pp. 159 – 180

Despite the general lack of unweathered Neogene outcrops in the Mecsek Mts., renewed efforts enabled palaeomagnetic sampling to be carried out at 29 localities of which 15 gave, after laboratory treatment, useful palaeomagnetic directions for the Ottnangian through Upper Pannonian.

Our results fall into four groups: (i) this group comprises the ignimbrites aligned with the northern margin of the Neogene sedimentary trough which exhibit counterclockwise rotated declinations averaging 60°; (ii) the younger sediments of the same trough with no rotation; (iii) Tertiary localities from the main Palaeozoic–Mesozoic body of the Mecsek Mts, where the Cretaceous alkali basalts and related rocks are characterized by declinations rotated to the east, exhibit similar easterly declinations; (iv) the declination of two Upper Pannonian localities from the surroundings of the Mecsek Mts. do not deviate significantly from the present north.

These results together with those from the Apuseni Mts. and the South Carpathians on one hand, and from the Slavonian Mts. on the other — all parts of the Tisza megatectonic unit — strongly suggest that this megatectonic unit was not yet a rigid body during the Tertiary as some tectonic models suggest.

The editor regrets the printing (software) error in the paper by E. Márton and P. Márton in the previous issue leading to the omission of the minus (–) sign in Tables I. and II. The corrected tables are enclosed.

Table I. Palaeomagnetic results for the igneous sites from the Mecsek Mts.
Explanation of symbols: Left column: identifying numbers (cf. text). n/n_0: useful collected number of samples. D and I: palaeomagnetic declination ($D°$) and inclination ($I°$) before tilt correction. k and $\alpha°_{95}$: statistical parameters after FISHER [1953]. k: precision, $\alpha°_{95}$: semi-angle of cone of confidence at the 95% confidence level. $D°_c$, $I°_c$: palaeomagnetic declination ($D°_c$) and inclination ($I°_c$) after tilt correction. *Dip*: bedding attitude, azimuth/magnitude of dip of bedding plane. *Remark*: *a*: result obtained by linearity analysis, *b*: result obtained from stable end points. Three results are shown for the Komló andesite (8). The first is from MÁRTON and MÁRTON [1969], the second is from MÁRTON [1986] and the third is from the present study. The last row shows an earlier result for an ignimbrite body from the Mid-Hungarian Zone [MÁRTON and MÁRTON 1989].

I. táblázat. A mecseki magmás kőzetek paleomágneses irányai.
Jelmagyarázat: bal oldali oszlop: azonosító számok (lásd szöveg), n/n_0: hasznos/gyűjtött minták száma, $D°$és $I°$: paeleomágneses deklináció és inklináció dőléskorrekció előtt; k és $\alpha°_{95}$: FISHER-féle [1953] statisztikai paraméterek; k: pontosság, $\alpha°_{95}$: a 95%-os megbizhatósági szintű konfidencia szög fele; $D°_c$, $I°_c$: paleomágneses deklináció és inklináció a dőléskorrekció után; *dip*: a tektonikai dőlés azimutja/a dőlés nagysága; *Remark*: *a*: linearitás analízissel kapott eredmény, *b*: stabil végpontokból kapott eredmény

	locality	n/no	$D°$	$I°$	k	$\alpha°_{95}$	$D°_C$	$I°_C$	k	$\alpha°_{95}$	dip	Remark
	Mecsek Mts. igneous rocks											
	Komló andesite* 1	10	82	+62	112	4						a
	Komló andesite* 2	5	71	+64	179	6						a
	Komló andesite* 3 7702–713	12/12	56	+59	164	3						a
8	Komló andesite mean	3	69	+62	143	10						
22	Kisbesztece ign. 7299–314	11/16	7	–67	67	6	105	–52	67	6	315/49	a
4	Horváthertelend ign. 7663–679	16/17	124	–53	33	7	84	–33	33	7	(220/40)	a
6	Vörösvölgy ign.	8/10	139	–33	15	15	99	–80	15	15	146/50	a
3	Balinca ign. 7417–425	9/9	67	–61	491	2	111	–59	491	2	351/26	a
7	Máza-Szászvár ign 6372–381	10/10	118	–57	35	8	118	–57	35	8	horizontal	a
	Mecsek ignimbrites overall mean	5	108	–62	8	28	113	–60	45	12		
	Mid-Hungarian Zone											
	Sárszentmiklós ignimbrite*	12/–	315	+55	47	7						

	locality	n/n_0	$D°$	$I°$	k	$\alpha°_{95}$	$D°_C$	$I°_C$	k	$\alpha°_{95}$	dip	Remark
9	Feked 7973–983	6/11	59	+55	22	17	62	+6	22	17	220/6	b
13	Mecsekjánosi 7602–611	5/10	191	+11	23	16	5	+79	23	11	10/89	a
12	Magyaregregy 7591-601, 7880–891	15/23	59	+74	120	3	355	+47	120	3	330/40	a
14	Orfű 7345–362	16/18	36	+58	43	6	19	+57	43	6	304/11	a
18	Komló-Kökönyös 7330–41	7/12	357	+53	126	5	350	+54	126	5	252/5	b
16	Husztót 7426–37	7/12	355	+63	25	12	4	+68	36	7	82/5 168/14	a
24	Danitzpuszta 7573–590	9/18	90	+60	19	12	118	+25	60	19	145/35	b
27	Bátaszék 7950–972	10/11	187	–61	136	4	201	–60	136	4	100/8	a
28	Kakasd 7892–901	5/10	193	–41	75	9	201	–46	75	9	135/10	a
	13, 12, 14, 18, 16 overall mean	5/5	24	+79	3	50	1	+61	34	13		

Table II. Palaeomagnetic results for sedimentary localities from the Mecsek Mts. *Explanation of symbols*: as for Table I.
II. táblázat. A mecseki üledékes kőzetek paleomágneses irányai. *Jelmagyarázat:* l. I táblázat alatt.

MAGYAR ÁLLAMI
EÖTVÖS LORÁND
GEOFIZIKAI INTÉZET

GEOFIZIKAI
KÖZLEMÉNYEK

ВЕНГЕРСКИЙ
ГЕОФИЗИЧЕСКИЙ
ИНСТИТУТ
ИМ Л. ЭТВЕША

ГЕОФИЗИЧЕСКИЙ
БЮЛЛЕТЕНЬ

GEOPHYSICAL

TRANSACTIONS

EÖTVÖS LORÁND GEOPHYSICAL INSTITUTE OF HUNGARY

CONTENTS

VOL. 43. NO. 1 MARCH 2000. (ISS N0016-7177)

BUDAPEST

TARTALOMJEGYZÉK

GEOPHYSICAL TRANSACTIONS 2000
Vol. 43. Number 1. pp. 3 – 18

Analysis of ground roll measurements based on a WKB solution of motion

Tamás FANCSIK*, Oszkár ÁDÁM*

During the past 20–30 years seismic ground roll lost a great deal of their significance because of the extensive use of geophone arrays, common depth points, etc. observation systems. Although with the help of these systems seismograms appear to be a great deal better the distortion effect of wave-guide generated ground roll has not eliminated from their frequency characteristics. This is connected to the viscoelastic phenomenon by velocity dispersion as well as absorption of *P* and *S* body waves. In this paper we deal only with velocity dispersion.

Keywords: ground roll, WKB solution, seismograms, P-waves, S-waves, velocity

1. Introduction

Ground roll — as is well known — was so-named because of its connection with reflection measurements. Because of its large amplitude ground roll can suppress the useful signals almost completely unless this disturbance is removed from seismograms. Detailed investigations relating to ground roll are contained in ÁDÁM's papers [1968, 1969] in which it was stated that the phenomenon can be considered as a mode of guided waves, due to the character of sedimentation of the near surface (mainly loess-like) layers with vertically increasing *P* and *SV* velocity distributions that can be considered continuous functions of the vertical co-ordinate. DOBRÓKA's [1987, 1988] and FANCSIK's [1995, 1997] publications have proved that the WKB approach can be applied for to describe the wave guide in an inhomogeneous medium. For this reason it seems to be useful to consider whether certain propagation characteristics of ground roll are explainable on the basis of the WKB solution of the motion equation valid in a vertically inhomogeneous medium. We shall examine this question in detail on the basis of experiments performed in the vicinity of Nagytilaj village (Zala County, Hungary) on the area of a loess plateau and compare the results with a modelling method described here. Acknowledge-

* Eötvös Loránd Geophysical Institute of Hungary, H-1145 Budapest, Kolumbusz u. 17–23
Manuscript received: 20 May, 1998.

ment is made to the Hungarian Scientific Research Fund (OTKA) grant No. 0155850.

2. Wave guide in vertically inhomogeneous medium

The ground roll mechanism is discussed on the basis of the full form in an inhomogeneous medium of the following motion equation:

$$\rho \frac{\partial^2 \vec{s}}{\partial t^2} = \mu \Delta \vec{s} + (\lambda + \mu)\,\mathrm{grad}\,\mathrm{div}\,\vec{s} + 2(\mathrm{grad}\,\mu, \mathrm{grad})\vec{s} + \\ + \mathrm{grad}\,\mu \times \mathrm{rot}\,\vec{s} + \mathrm{grad}\,\lambda\,\mathrm{div}\,\vec{s} \tag{1}$$

where λ and μ are Lamé's constants, ρ is the density.

In the case of two-dimensional wave propagation, by means of the displacement potentials ($\vec{s} = \nabla\varphi + \mathrm{rot}\,\vec{\psi}$, φ is the scalar potential; $\vec{\psi} = \{0, \psi, 0\}$ is the vector potential) this relation is reducible to easily solvable form by the WKB method [FANCSIK 1995, 1997]:

$$\Delta\varphi + k_\alpha^2 \varphi = -\frac{2}{\xi}\frac{\mathrm{d}\mu}{\mathrm{d}z}\frac{\partial\psi}{\partial x} \\ \Delta\psi + k_\beta^2 \psi = \frac{2}{\mu}\frac{\mathrm{d}\mu}{\mathrm{d}z}\frac{\partial\varphi}{\partial x} \tag{2}$$

(k: wave number; $\xi = \lambda + 2\mu$). The wave propagation was supposed in the (x, z) plane (then only the x and z direction components of the displacement vector exist), and the density of the medium was considered constant. The equations are valid only for fulfilling the following inequalities:

$$|\,\mathrm{grad}\,\varphi\,| \gg \left| \frac{2}{\rho\omega^2} \{(\mathrm{grad}\,\varphi, \mathrm{grad})\,\mathrm{grad}\,\mu - \mathrm{grad}\,\varphi\,\Delta\mu\} \right| \\ |\,\mathrm{rot}\,\vec{\psi}\,| \gg \left| \frac{2}{\rho\omega^2} (\mathrm{rot}\,\vec{\psi}, \mathrm{grad})\,\mathrm{grad}\,\mu \right| \tag{3}$$

where ω is the angular frequency.

The λ, μ Lamé coefficients depend only on the z co-ordinate and in the case of two dimensions we can disregard the derivative from the y direction. Equations $k_\alpha = \omega/\alpha(z)$ and $k_\beta = \omega/\beta(z)$ are the wave numbers of body waves (where $\alpha(z)$, $\beta(z)$ are respectively the velocities of the longitudinal and the transversal body wave). The displacement components of these waves fall in the (x, z) plane too. According to the inhomogeneities of layer series the rela-

tions of equations (2) are valid, the *P*- and *SV*-waves became coupled waves. Naturally the horizontally polarized transversal (*SH*) wave appears too, but from our present point of view it is not of interest.

The conditions of inequalities given by equations (3) are trivially fulfilled if dependence of the Lamé coefficients is assumed to be linear in space, that is $\mu=\mu_0(1 + az)$, $\lambda=\lambda_0(1+az)$, where μ_0, λ_0 are values of the Lamé coefficients in the $z=0$ plane, and a is the parameter determining the rate of inhomogeneity (namely equations (3) contain only second derivatives). In this case the velocities of waves in the medium will vary according to the 1/2 power of the z depth and the gradient of $V(z)$ is continuously decreasing. In this way we shall get such a velocity distribution which has a decreasing gradient with depth and will approach the often experienced velocity courses caused by the compression within the near-to-surface geological structures [ÁDÁM 1968].

On the basis of the WKB solutions of equations (2) the components of the displacement vector in a vertically inhomogeneous medium will be as follows [FANCSIK 1997]:

$$u_x = \left(\mathrm{i}ka(z)A\mathrm{e}^{-\int_z^{} p(y)\mathrm{d}y} + qb(z)C\mathrm{e}^{-\int_z^{} q(y)\mathrm{d}y} + \mathrm{i}ka(z)B\mathrm{e}^{\int_z^{} p(y)\mathrm{d}y} - qb(z)D\mathrm{e}^{\int_z^{} q(y)\mathrm{d}y} \right) \mathrm{e}^{\mathrm{i}kx}$$

$$u_z = \left(-pa(z)A\mathrm{e}^{-\int_z^{} p(y)\mathrm{d}y} + \mathrm{i}kb(z)C\mathrm{e}^{-\int_z^{} q(y)\mathrm{d}y} + pa(z)B\mathrm{e}^{\int_z^{} p(y)\mathrm{d}y} + \mathrm{i}kb(z)D\mathrm{e}^{\int_z^{} q(y)\mathrm{d}y} \right) \mathrm{e}^{\mathrm{i}kx} \tag{4}$$

where

$$p=\sqrt{k^2-k_\alpha^2}, \quad q=\sqrt{k^2-k_\beta^2}, \quad a(z)=\sqrt{p_0/p}, \quad b(z)=\sqrt{q_0/q},$$

k is the wave number to the x direction and we disregarded from the above-mentioned coupling effect; A, B, C, D are arbitrary coefficients. The members with the zero subscript relate to one of the fixed points of the layer, e.g. to the $z=0$ point of co-ordinates. The fulfilment of these equalities according to the WKB solution implies new conditions; with the notations

$$P(z,f)=\left|\frac{1}{p^{5/2}}\left(\frac{3}{4}\left(\frac{1}{p}\frac{\mathrm{d}p}{\mathrm{d}z}\right)^2-\frac{1}{2}\frac{1}{p}\frac{\mathrm{d}^2p}{\mathrm{d}z^2}\right)\right|$$

and

$$Q(z,f)=\left|\frac{1}{q^{5/2}}\left(\frac{3}{4}\left(\frac{1}{q}\frac{\mathrm{d}q}{\mathrm{d}z}\right)^2-\frac{1}{2}\frac{1}{q}\frac{\mathrm{d}^2q}{\mathrm{d}z^2}\right)\right|$$

They will take the following shape

$$P(z, f) << 1$$
$$Q(z, f) << 1 \tag{5}$$

On interpreting equations (4) one can see that in a vertically inhomogeneous medium, such *P*- and/or *SV*-waves can develop which, for example, starting from a free surface will return to the free surface in case of certain incidence angles. These are *diving-waves,* that characterize loose sediments. *Figure 1* models an often occurring near surface geological situation from the point of view of a wave-guide. In the figure a vertically inhomogeneous, low velocity layer lies on a rock body that can be considered as an infinite half space in which the longitudinal and the vertical body wave velocities, depending on the given location and density, are constant. Consider H the thickness of this layer. This layer having lower *SH*-wave velocity (by chance *P*-wave velocity) compared with the half space is the wave guide channel in which — if the channel was homogeneous — a guided wave built of reflected waves from

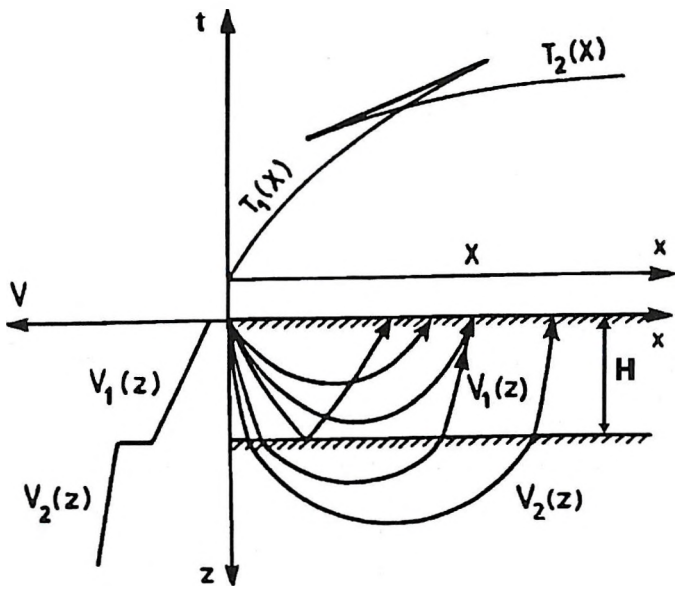

Fig. 1. Theoretical ray combination in the case of diving waves. Two layers with different *V(z)* characteristics

1. ábra. Elméleti sugárkombináció bemerülő hullámok esetén. Két réteg eltérő *V(z)* karakterisztikákkal

the surface and the basement would propagate parallel with the surface. According to the above interpretation, but for an inhomogeneous case, besides the reflected waves such waves (*P*- and/or *SV*-waves) also appear in the upper layers that will not reach the surface of the lower half space and in this way they return to the free surface. Thus the wave guide developing in the inhomogeneous medium differs from the wave guide developing in a homogeneous, two-layer case when it is not necessary to take into account the wave propagation as a diving wave or the frequent reflections (on the surface) of these waves.

In order to examine the wave-guide in an inhomogeneous medium, the two-layer model of Fig. 1 should also be taken into account in the following. In the layer of finite thickness, displacements given by equations (2) are valid. Moreover, consider the lower half space as an inhomogeneous one in which the following functions will give the displacement components (marking the par-ameters relating to the second layer with a prime):

$$\begin{aligned} u'_x &= \left(\mathrm{i}kE\,\mathrm{e}^{-p'z} + q'F\,\mathrm{e}^{-q'z}\right)\mathrm{e}^{\mathrm{i}kx} \\ u'_z &= \left(-p'E\,\mathrm{e}^{-p'z} + \mathrm{i}kF\,\mathrm{e}^{-q'z}\right)\mathrm{e}^{\mathrm{i}kx} \end{aligned} \tag{6}$$

E, F are arbitrary constants.

In this layer only the *P-SV*-waves travelling outward in the direction of the *z*-axis were taken into account at the resolution (which is given on the basis of the regularity condition). The functions

$$p' = \sqrt{k^2 - k_\alpha'^2}, \quad q' = \sqrt{k^2 - k_\beta'^2}$$

are direction cosines. In a layered medium the waves given by displacement components (2) and (6) should fulfil the boundary conditions:

— the normal components of the stress will disappear on the surface;

— at depth *H*, on the boundary of the two layers the appropriate displacement components (of *x* and *z* direction) and normal stress are continuous;

— in the lower half space in case of $z \to \infty$ the regular solution of wave equation can be get.

If we write these conditions for the integration constants *A, B, C, D, E, F* as unknown coefficients we shall get a homogeneous, linear equation system. On the basis of this system of equations we arrive to the dispersion relation of *P-SV*-waves propagating in a vertically inhomogeneous medium as follows:

$$\det(\underline{\underline{MN}}) = 0 \tag{7}$$

where

$$\underline{M} = \begin{pmatrix} \mathrm{i}ka & qb & \mathrm{i}ka & -qb & +\mathrm{i}k & -q' \\ -pa & \mathrm{i}kb & pa & \mathrm{i}kb & p' & +\mathrm{i}k \\ -2\mathrm{i}kp\mu a & -\mu(k^2+q^2)b & -2\mathrm{i}kp\mu a & -\mu(k^2+q^2)b & 2\mathrm{i}kp'\mu' & -\mu'(k^2+q'^2) \\ (p^2\xi - k^2\lambda)a & -2\mathrm{i}kq\mu b & (p^2\xi - k^2\lambda)a & 2\mathrm{i}kp\mu b & +(p'^2\xi' - k^2\lambda') & 2\mathrm{i}kq'\mu' \\ -2\mathrm{i}kp\mu e & -\mu(k^2+q^2)/f_s & -2\mathrm{i}kp\mu/e & -\mu(k^2+q^2)/f_s & 0 & 0 \\ (p^2\xi - k^2\lambda)e & -2\mathrm{i}kq\mu b f_s & (p^2\xi - k^2\lambda)/e & 2\mathrm{i}kq\mu/f_s & 0 & 0 \end{pmatrix}$$

$$\underline{N} = \mathrm{diag}\ 1/e \quad 1/f_s \quad e \quad f_s \quad g \quad h)$$

$$e = \exp\left(\int_0^H p(y)\,\mathrm{d}y\right), \quad f_s = \exp\left(\int_0^H q(y)\,\mathrm{d}y\right), \quad g = \exp(+p'H), \quad h = \exp(+q'H),$$

$$\xi = \lambda + 2\mu, \quad \xi' = \lambda' + 2\mu'.$$

The values of a and b are of the WKB amplitude correction at depth H given in connection with equation (4).

On analysing the results of field registration by means of equation (7) we investigate the conformity of phase velocities supplied by the field registrations and determined from modelling.

3. Comparison of results of ground roll measurements and results of modelling

The experimental ground roll measurements were carried out in the above mentioned region near to Nagytilaj, where the surface waves were generated by vertical force (by shot) on the surface; the observation was by means of geophones of horizontal and vertical orientation and linear phase digital system-equipment corresponding to the direction of the seismic line. *Figure 2* shows the seismogram where different wave groups can be distinguished. In order to determine the dispersion relations of the waves *f–k* analyses have been performed the results of which can be found in *Fig. 3.* The c_1, c_2 and c_3 phase velocity courses which can be determined on the basis of the curves marked f_1, f_2 and f_3 are indicated respectively by empty squares, empty triangles and empty circles in *Fig. 4.* We represented the *f–k* curves and phase velocities of those waves which support the largest ratio of the energy propagating in the wave-guide.

In order to apply dispersion relation (7), a geological model of the wave-guide will be required. In the experimental measurement for clarifying the geological relations and the physical parameters, velocity and density profil-

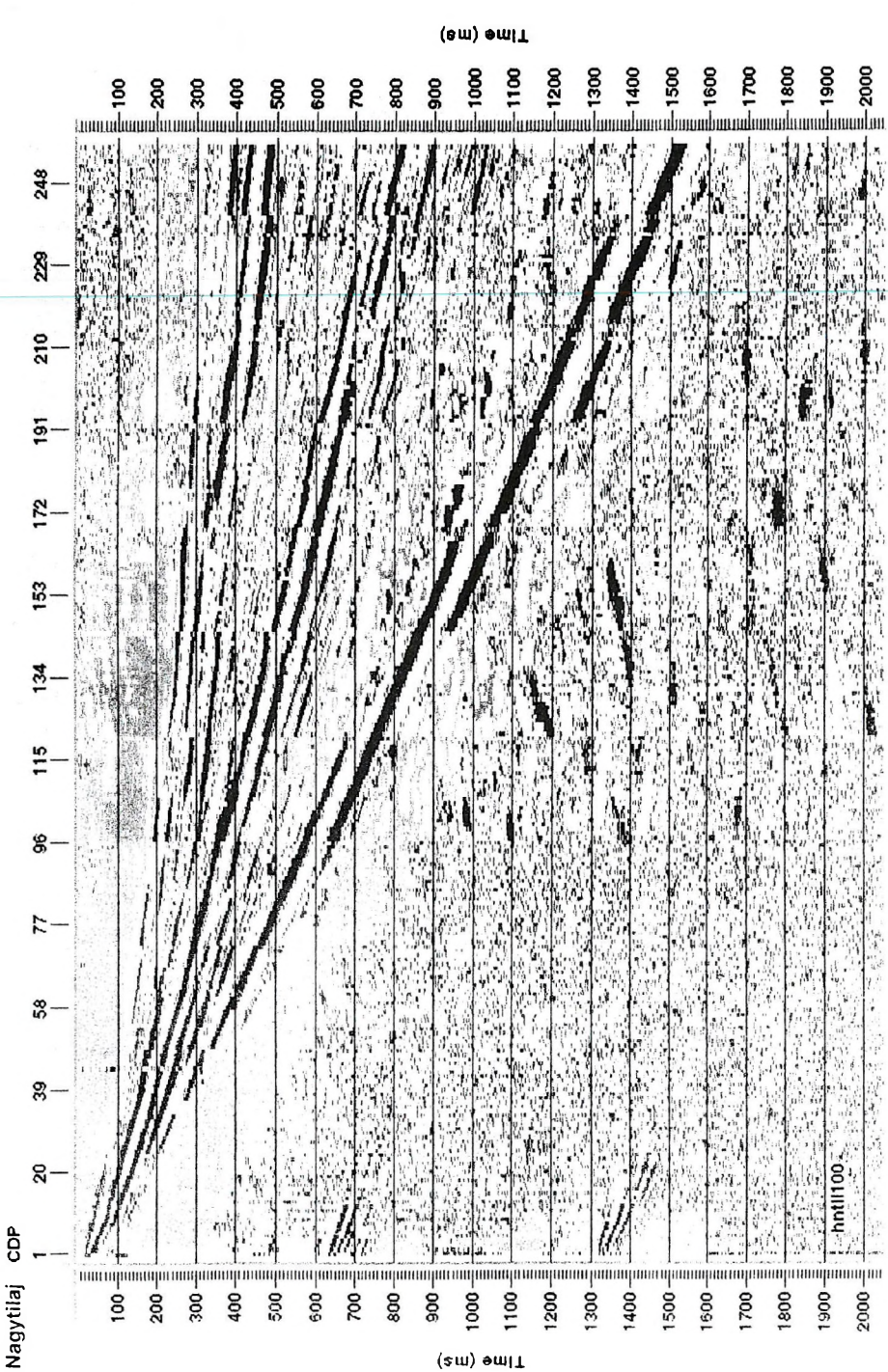

Fig. 2. Seismogram from Nagytilaj area observed with 254 vertical geophones, Δx=1m; L=254 m

2. ábra. Szeizmogram Nagytilajból. 254 geofon, Δx=1m, L=254 m

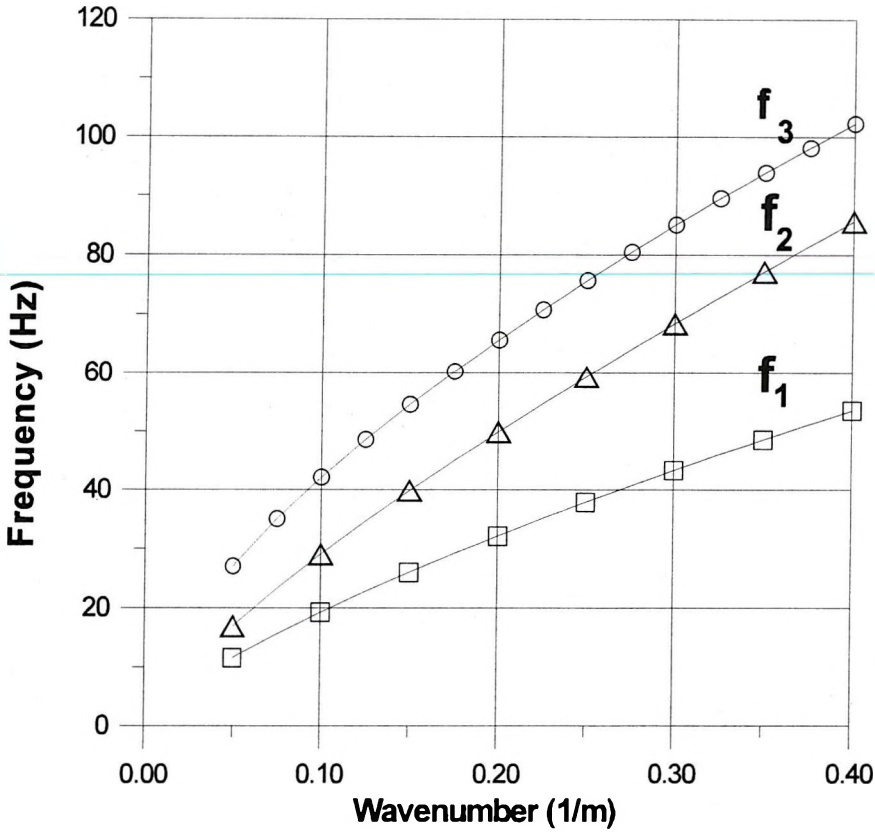

Fig. 3. Results of *f–k* analysis for the different time–distance curves
3. ábra. Az *f–k* analízis eredményei különböző idő–távolság görbékre

ing were performed as a means of determining the distribution by depth of the *P*- and *S*-waves as well as the density. In addition, data from the first break registrations were processed.

Assessment of the results of seismograms indicated that the thickness of the layers is approximately 40 m, meaning a significant *P*- and *S*-wave velocity gradient. Below this thickness, from the aspect of propagation of the longitudinal wave there is however a consolidated layer. The transversal wave velocity in this layer can be considered as a location-dependent one. The parameters of the model of the wave-guide are given in *Table I.*

V_P (m/s)	V_S (m/s)	Density (kg/m^3)	Thickness of layer (m)
$228\sqrt{1+0.3z}$	$115\sqrt{1+0.3z}$	2000	40
1900	1100	2300	–

Table I. Model of wave-guide formed on the basis of the field measurements. V_P means the longitudinal body wave velocity, V_S the transversal body wave velocity. The parameters of the upper layer are shown, and the bottom line gives the values of the half space considered to be consolidated

I. táblázat. A terepi mérések alapján kialkított hullámvezető modell. V_P a longitudinális, V_S a transzverzális térhullám sebessége. A második sor a felső réteg paramétereit, az alsó sor a konszolidáltnak tekintett féltér értékeit adja

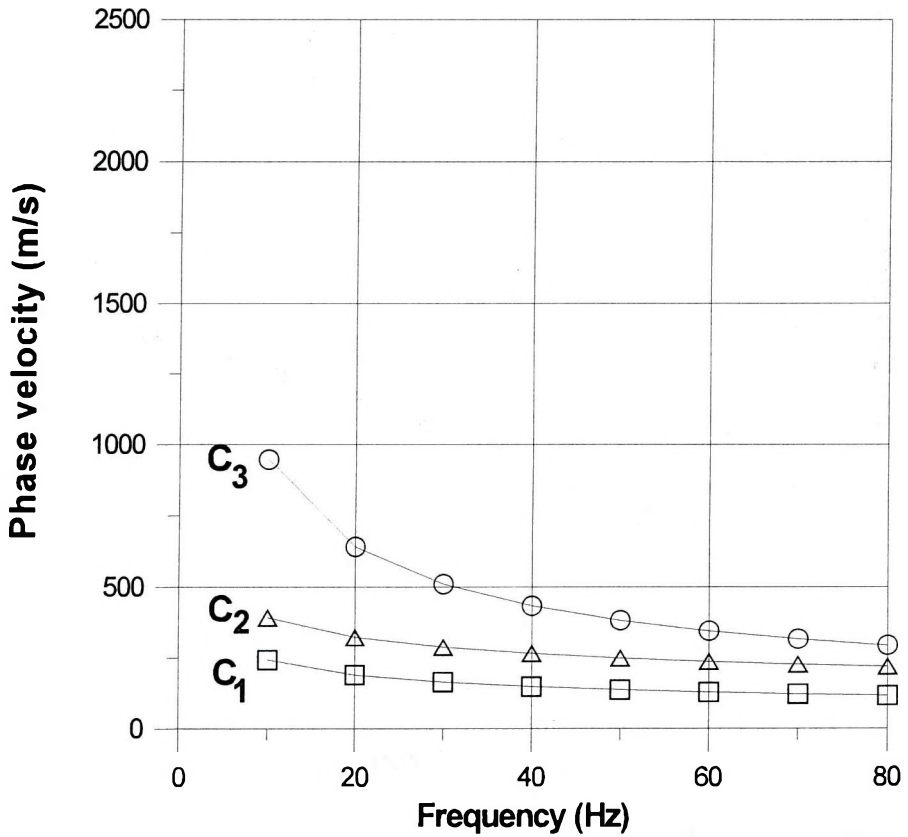

Fig. 4. Dispersion curves computed from curves of Fig. 3

4. ábra. A 3. ábra görbéiből számított diszperziós görbék

This form of $V = V_0\sqrt{1+az}$ is the velocity approximation determined from the field measurements (the validity of the WKB approximation will be proved later). In *Fig. 5* the velocity–depth curve supplied by this function for transversal body wave velocity is presented. (In the figure we also presented the $V=Az^{1/n}$ form velocity equation that proved good in practice [ÁDÁM 1968] and that was applied in this region too and the parameters of which were A=113/s, n=2.82 on the basis of observation). In the lower half space the transversal wave velocity was regarded as constant on the one hand because the variability of V_S is lower in this range than that experienced in the upper layer

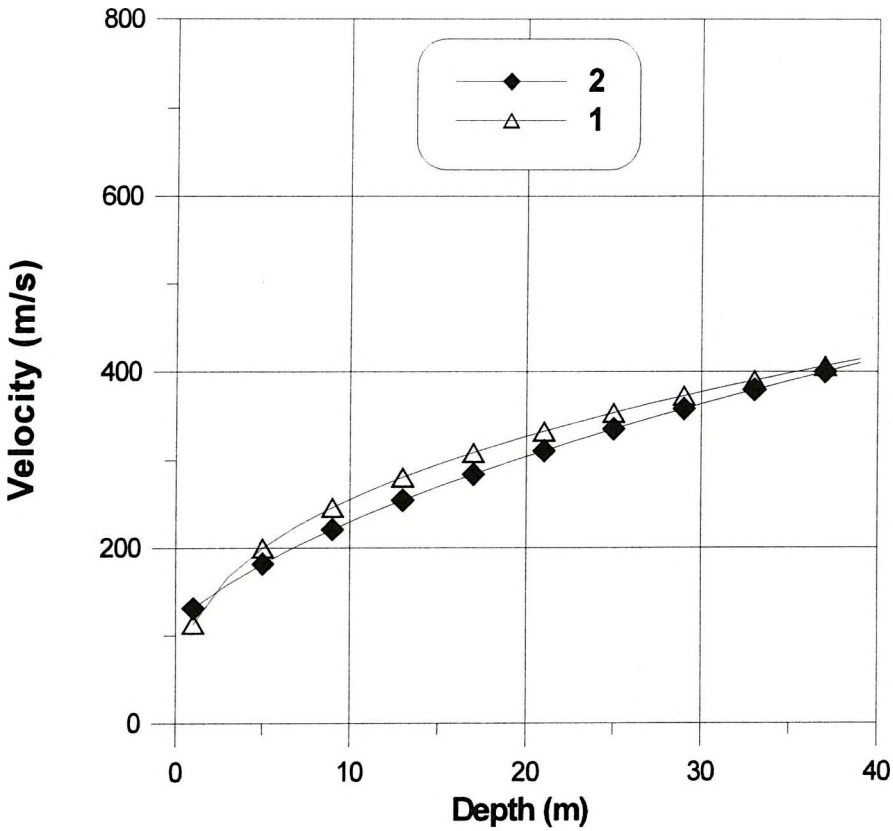

Fig. 5. V(z) velocity–depth curves. *Curve 1*: $V = V_0\sqrt{1+az}$ simplified from well velocity survey ; *curve 2*: computed from surface measurement $V=Az^{1/n}$

5. ábra. V(z) sebesség–mélység diagram.

1. görbe: fúrólyukban mért sebességfüggvény egyszerűsített formája $V = V_0\sqrt{1+az}$;

2. görbe: felszíni mérésekből számított görbe $V=Az^{1/n}$

and on the other hand the wave guide connects to the near-to-surface layer that shows more significant inhomogeneity [ÁDÁM 1987], namely the propagation characteristics of the guided wave connecting to the near-to-surface are influenced into a smaller extent by the velocity relations of the deeper ranges.

On the basis of the model given above the dispersion curves plotted by using dispersion relation (7) can be found in *Fig. 6* (curves marked with filled circles, triangles and squares) where also the dispersion curves derived from the ground data shown in Fig. 2 are indicated (with empty circles, triangles and squares). It can be seen that the curves from the measurements and the modelling lie together essentially in the examined frequency range. A difference can be observed mostly for the middle velocity branch. The degree of fit relating to a pair of curves can be characterized numerically too, for example

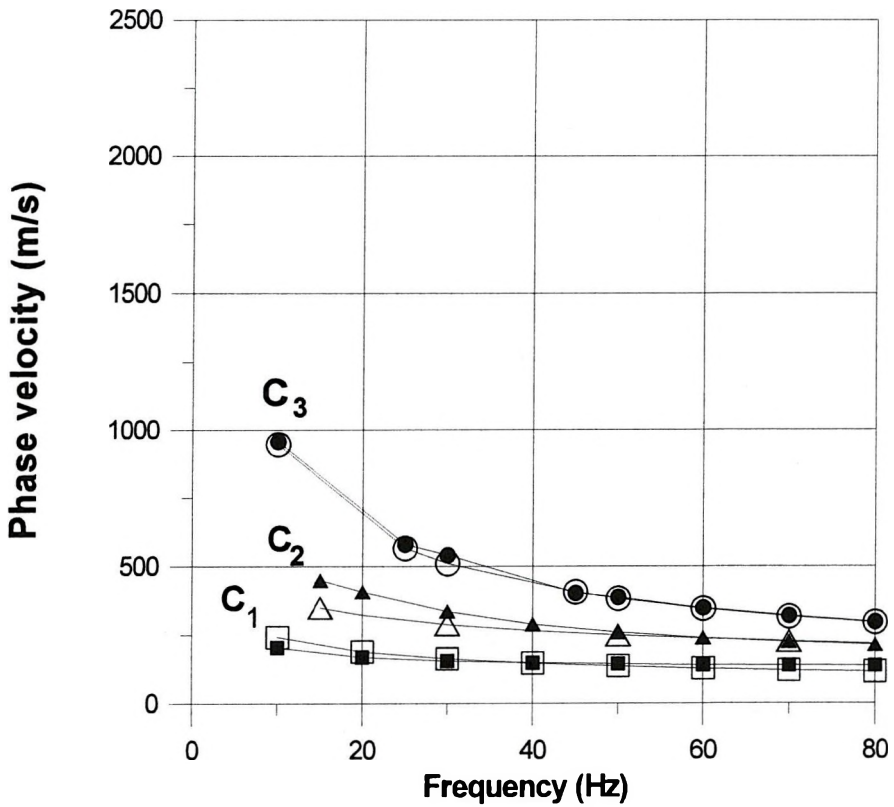

Fig. 6. Measured and computed phase velocities
6. ábra. Mért és számított fázissebességek

by means of the relative errors of the two curves according to the following formula:

$$\varepsilon_a = \sqrt{\frac{1}{N}\sum_{i=1}^{N}\left(\frac{c_i^{(m)} - c_i^{(sz)}}{c_i^m}\right)^2} \quad , \tag{8}$$

where ε_a is the 'standard deviation' of relative errors of the plotted $c_i^{(m)}$ and calculated $c_i^{(sz)}$ phase velocities for the same N frequencies as the parameter characterizing the average fit. Using this formula the degree of fit for the single curves is as follows (*Table II*):

Velocity curve	ε_S(%)
c_3	2.4
c_2	15
c_1	11

Table II. The degree of fit of the phase velocities plotted on the basis of velocity curves marked c_1, c_2, and c_3 presented in Fig. 4 as well as the dispersion relation formula (7) and the parameters of Table I according to formula (8)

II. táblázat. A 4. ábrán megadott c_1, c_2 és c_3 jelű sebsséggörbék, valmint a diszperziós egyenlet (7) és az I. táblázat paraméterei alapján számított fázissebességek illeszkedésének mértéke a (8) egyenletnek megfelelően

Bearing in mind the measuring errors as well as the accuracy of the two-layer model (that simplifies the reality) formed on the basis of the above statements, the results of the modelling can be considered satisfactory.

The results of the WKB modelling could be accepted if the conditions of the WKB approximation are fulfilled in the frequency range examined. Since the validity of inequalities (3) is trivial due to the above selection of shape of the velocity functions only the validity of the pair of inequalities (5) should be examined.

Regarding the above requirement by means of the results in *Figures 7* and *8* we would like to demonstrate the response of $P(z, f)$ and $Q(z, f)$ as functions of frequency and of depth relating to unity (marking unity with a thick line in the figures) in the case of velocity curve c_1 (marked with squares in Figure 4) at three different depths. On the basis of the figures it is evident that the results of the WKB modelling are valid for higher frequencies than 20 Hz. It is mentioned that the consequence will also be the same for the further two phase velocity functions.

With regard to the ground roll registrations measured in the Nagytilaj region: on the basis of the results obtained from dispersion equation (7) we can state that ground roll can be considered as a higher mode of *P-SV* guided waves. The lowest velocity mode (marked with circles in Figures 3 and 4) is the first overtone following the Rayleigh type wave propagating in the medium. (In this case, by Rayleigh type wave we mean the dispersion fundamental harmonic which at low frequency approaches the Rayleigh wave velocity of the half space considered consolidated and by increasing the frequency it approximates the Rayleigh wave velocity of the layer of finite thickness.) On the basis of the velocities from dispersion analysis and the displacement functions given by (4) it can also be stated that the displacement components of the ground roll are built of displacement components of *SV*-waves propagating as a diving one and as of inhomogeneous *P*-waves. The neglecting of coupling did not lead to significant errors.

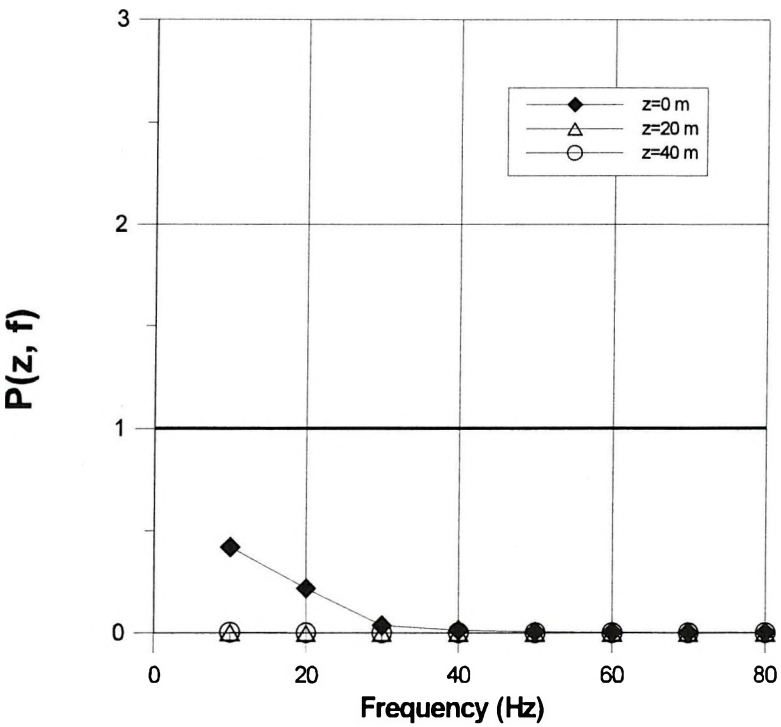

Fig. 7. Value of *P (z, f)* as a measure of the approximation
7. ábra. P (z, f) értéke mint a közelítés mértéke

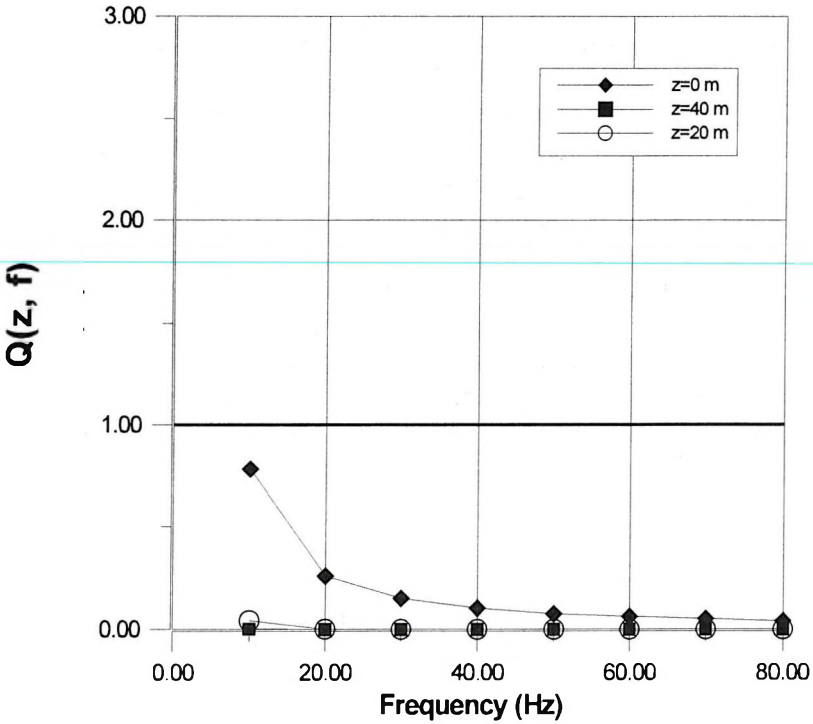

Fig. 8. Value of $Q(z, f)$ as a measure of the approximation
8. ábra. $Q(z, f)$ értéke, mint a közelítés mértéke

4. Summary

On the basis of the WKB approximation of the motion equation in an inhomogeneous medium we gave the dispersion relation of *P-SV*-waves propagating in such a two-layer, near-to-surface structure where the layer of finite thickness situated on a half space considered homogeneous was considered vertically inhomogeneous. Using these results we derived the phase velocities of the *P-SV*- waves relating to that wave guide model whose determination occurred on the basis of seismic and well-log measurements. Comparing our curves with the phase velocity curves — derived from dispersion analysis — of ground roll measurements performed in the above-mentioned region we are able to state appropriate coincidence in the examined frequency range. However this frequency range was determined by the terms relating to the validity of the WKB approximation. From the results the following consequence was drawn. In the given area, surface ground roll is the higher mode of such *P-SV*

guided waves whose displacement components are built of displacement components of *SV*-waves propagating as immersion waves as well as of inhomogeneous *P*-waves.

The above presented WKB modelling of the dispersion relation of ground roll as a *direct solution* gives the possibility that in future the examination of seismic parameters of near-to-surface structures should be performed by the inversion technique based on this measuring method, a method that may prove to be of great importance in resolving various environmental, geotechnical or geophysical engineering tasks.

REFERENCES

ÁDÁM O. 1968: Surface ground roll. (in Hungarian) Magyar Geofizika **IX**. 2. pp. 41–53

ÁDÁM O. 1969: Analysis of the seismic ground roll. Acta Geodaet., Geophys et Montanist. Acad. Sc. Hung. **4**, pp. 95–133

ÁDÁM O. 1987: Seismic research. I-II. (in Hungarian) Tankönyvkiadó, Budapest 632 p.

DOBRÓKA M. 1987: Love seam waves in a horizontally inhomogeneous layered medium. Geophysical Prospecting **35**, pp. 502–516

DOBRÓKA M. 1988: On the absorption-dispersion characteristics of channel waves in coal seams of varying thickness. Geophysical Prospecting **36**, pp. 318–331

FANCSIK T. 1995: Dispersion relation and displacement functions of P-SV-waves propagating in laterally slightly inhomogeneous medium. (in Hungarian) Magyar Geofizika **36**, 3, pp. 215–221

FANCSIK T. 1997: Examination of the dispersion relation of Rayleigh type waves propagating in a wave guide characterized by layer parameters depending slightly on location. (in Hungarian). Candidate thesis, Hungarian Academy of Sciences, Budapest, (manuscript)

Felszíni zavarhullám mérések analízise a mozgásegyenlet WKB megoldása alapján

FANCSIK Tamás és ÁDÁM Oszkár

Az elmúlt 20–30 évben a szeizmikus zavarhullám (seismic ground roll) jelensége annyiban veszített jelentőségéből, amennyiben a hosszú geofon csoportok és nagy fedésszámú észlelési rendszerek segítségével nagyrészt elnyomták. Bár az ezekkel az észlelési rendszerekkel felvett időszelvényeket kevésbé terhelik a hullámvezetőkben keletkező zavarhullámok, de hatásuk a frekvencia karakterisztikákban továbbra is él. Ehhez kapcsolódnak a viszko-elasztikus kőzetmodellre jellemző abszorpció és diszperzió, amelyek mind a *P*, mind az *S* hullámot terhelik. Ebben a dolgozatban csak a *sebesség diszperzióval* foglalkozunk.

ABOUT THE AUTHORS

Tamás Fancsik (1968) graduated at the University of Miskolc in 1992. After graduation he commenced work as a scholarship holder within the University's Department of Geophysics. Since 1996, he has been working for Eötvös Loránd Geophysical Institute of Hungary. The topic for his Ph.D. (awarded in 1998) was the dispersion of P-SV guided waves in inhomogeneous medium. His current research, from the field of deep reflection seismology, includes data processing, rheology, and the attenuation and energy dissipation of seismic waves.

Oszkár Ádám (1927) graduated as a mining engineer from the University of Heavy Industry, Miskolc. From 1950–56, he was engaged in oil, coal and other mineral surveys on the territory of Hungary; from 1956–62, he carried out oil and gas prospecting in the People's Republic of China. As an expert in seismic prospecting, he was an invited lecturer at Miskolc University from 1960–1996. For over 20 years (1964–1987) he was head of the exploration department of Hungary's Central Geological Office. He is a member of the Association of Hungarian Geophysicists and the European Association of Exploration Geophysicists.

GEOPHYSICAL TRANSACTIONS 2000
Vol. 43. Number 1. pp. 19 – 31

Dispersion analysis of ground roll using analytical velocity functions

Oszkár ÁDÁM* and László HERMANN*

Seismic ground roll is a characteristic feature of area covered by loose loess sediments. On these areas mainly the velocity distribution is depth dependent and can be approximated by analytical functions. If the characteristic features of these sediments are the velocity dispersion and the absorption these can be considered to provide a visco-elastic rock model. We should like to support this hypothesis by analysing the results of our field experiments and modelling.

Keywords: dispersion, ground roll, velocity

1. Introduction

Since the beginning of the intensive seismic prospecting in Hungary, but particularly between 1953 and 1968, many experiments were carried out in an endeavour to learn about the nature of the most disturbing wave — *ground roll* — which causes the so called *no reflection (NR)* areas. These were the hilly part of Transdanubia, and several smaller local territories of the Great Hungarian Plain [ÁDÁM 1954, 1964; SZÉNÁS, ÁDÁM 1953; ÁDÁM, Sz.KILÉNYI 1963; ÁDÁM 1969]. After this rather long period and because of the technological–methodological development based on computerization, miniaturization of equipment, the *common depth point (*CDP) system and geophone arrays used in the field, ground roll became only a memento to the seismologists and not an object to study in detail. One of the most interesting publications in this respect was that of ANSTEY *[Whatever happened to ground roll?* 1986].

Since 1986 three other papers should be mentioned here: GABRIELS et al. [1987] investigating the dispersion characteristics of a sand layer series on a flat area of a beach; KRAGH et al. [1995] proposing the use of the elliptical nature of ($\mathbf{u}_x$, $\mathbf{u}_z$) displacements or ($\mathbf{v}_x$, $\mathbf{v}_z$) displacement velocity amplitudes of ground roll; SCHNEIDER, DRESEN [1994] who used the dispersion characteristics of ground roll to determine the depth variation of a shallow refuse pit. All

* Eötvös Loránd Geophysical Institute of Hungary, H-1145 Budapest, Kolumbusz u. 17–23
Manuscript received: 30 April, 1998.

three publications consider ground roll as different modes of Rayleigh type or at least *P-SV*-waves. Our aim is to give more information about the nature of ground roll with regard to dispersion.

2. Field investigation

During the last three years we had the opportunity to carry out field investigations on an area of *no reflections* or *very poor reflections*. Data acquisition was carried out by parameters (254 m long spread, 1 m geophone interval, vertically effective force as source) suitable for *f–k* analyses and determination of dispersion characteristics of the layer series consisting of loose sediments such as different kind of loesses and upper Pannonian clayey sands, etc.

A very important property of these sediments is the compressibility that involves the *V(z)* depth dependence of any kind of seismic (*P*- and *S*-) wave velocities. The thickness of these dry formations is generally about 30–50 m above the watertable, but at some places much more. In consequence of these situations the seismograms were built up of disturbing *ground roll* waves (*Fig. 1*) suppressing and damaging all the reflection signals by their very large amplitudes, and generating different kinds of other noises (for example different kind of harmonics), too. The effect of depth dependent velocity variations is apparent by the *diving wave* character. On the seismogram the curvilinear character of different group of arrivals and the widening trains of disperse waves can be clearly seen. These also mean that 100 or more folds of common depth point spreads had or have to be used to obtain a fairly good time section. Because of the consistency of these loose sediments, the validity of a *visco-elastic solid model* is supposed. This was comprehensively analysed by RICKER [1953]. Judging from this model the main features of elastic waves are the *dispersion and frequency dependent attenuation.* DOBRIN [1951], TOLSTOY and USDIN [1953], ÁDÁM [1969] gave some proof of this behaviour. The present paper deals solely with the dispersion characteristics of *ground roll* but in somewhat more detail.

3. Fitting of seismic parameters

In order to describe the velocity–depth relation some simple analytical functions were used in seismic prospecting [BANTA 1941, WHITE 1963, KAUFMAN 1953, and, recently, AL-CHALABI 1997]. For example the more simple ones are

$$V(z) = V_0 (1+kz)^{(1/n)} \tag{1}$$

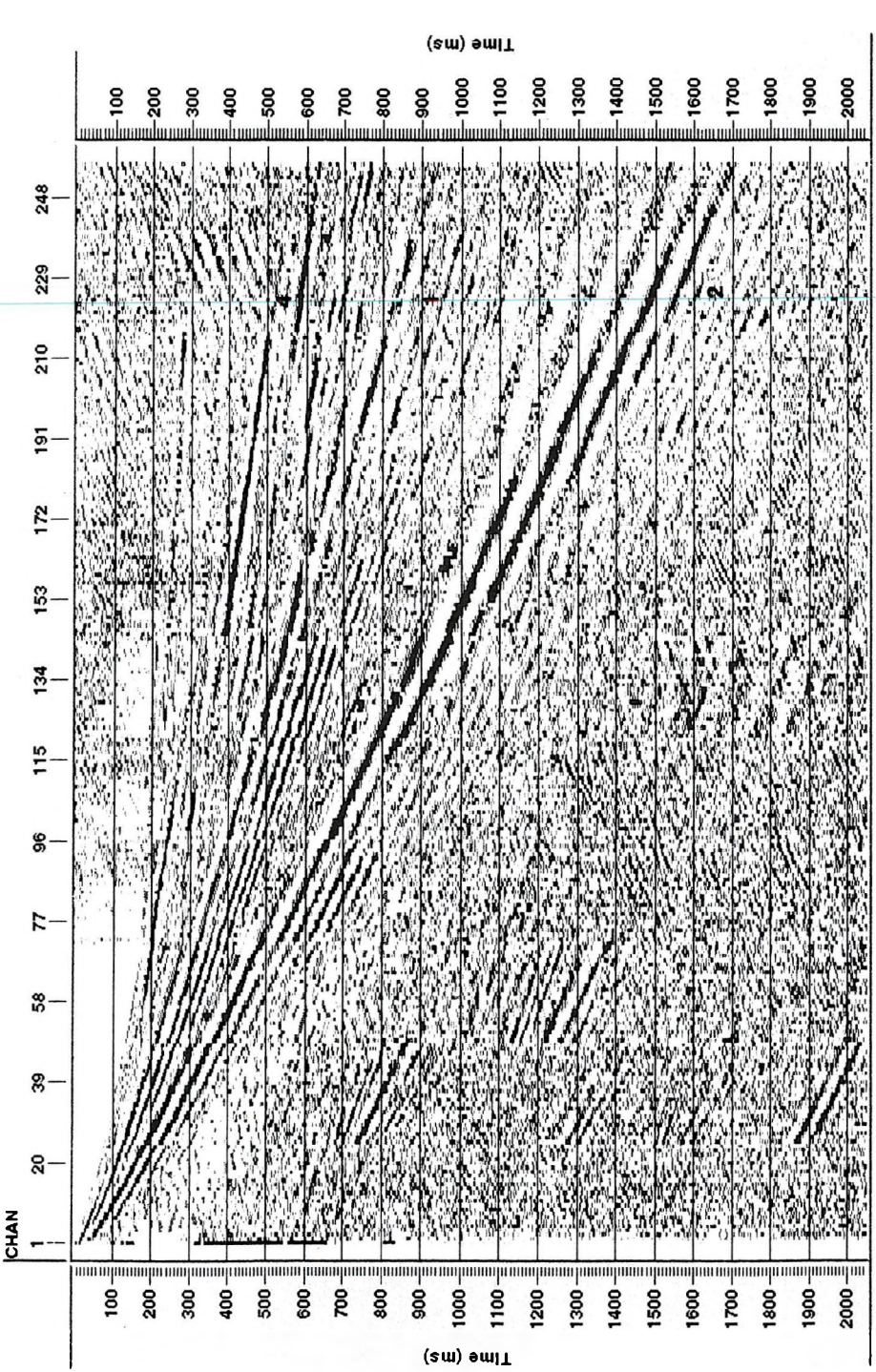

Fig. 1. Ground roll seismogram from Hungary's Udvari region (Tolna County)
1. ábra. Zavarhullám szeizmogram az Udvari (Tolna m.) területről

$$V(z)=A\,z^{(1/n)} \tag{2}$$

$$V(z)=V_0 \exp(-kz) \tag{3}$$

(The dimensions are: V(m/s); A(1/s); n (dimensionless); z(m); k(1/m))

If we suppose the validity of one of these power functions, e.g. equation (2), the travel times can be approximated by a relatively simple equation, as follows:

$$t(x)=\frac{n\pi^{\frac{1}{2}}}{A}\frac{\Gamma\left(\frac{n-1}{2}\right)}{\Gamma\left(\frac{n}{2}\right)}\left[\frac{x\Gamma\left(\frac{n}{2}+1\right)}{n\pi^{\frac{1}{2}}\Gamma\left(\frac{n+1}{2}\right)}\right]^{\frac{n-1}{n}} \tag{2a}$$

where Γ is the well known gamma function, A is a parameter with dimension of 1/s, n is a dimensionless constant. The parameters of velocity function (2) are A and n and these can be computed from the travel time equation. For Fig.1 this means at least three for the different groups of waves.

The *f–k* diagram (*Fig. 2*) has the characteristics of a power function, too, like *t(x)* travel-time on Fig. 1. Based on our own experience *the velocity function of type (2) is a good approximation and therefore the C(f) phase velocity–frequency relation of the ground roll* can in many cases be described quite well in the form of

$$C(f)=C_1 f^{-m} \tag{4}$$

where $m < 1$, C_1 is a constant *(Fig. 3)*.

From what is described above one can conclude that the depth dependence of seismic parameters (i.e. the $V_P(z)$, $V_S(z)$ propagation velocities and the $\rho(z)$ density) in such cases can also be described by simple analytical functions. The application of this kind of function has some advantages because

— the main features of data are represented
— the relations between *C(f)* and *V(z)* data are clearly shown
— the large computational efforts of inversion tasks can considerably be reduced.

According to the well-log data the density–depth function can be described in the form of

$$\rho(z)=\rho_v-(\rho_v-\rho_0)\exp(-Kz) \tag{5}$$

Where for the first layer $\rho_0=\rho(0)$, $\rho_v=\rho(\infty)$, K determines the gradient of the density function $\rho(z)$.

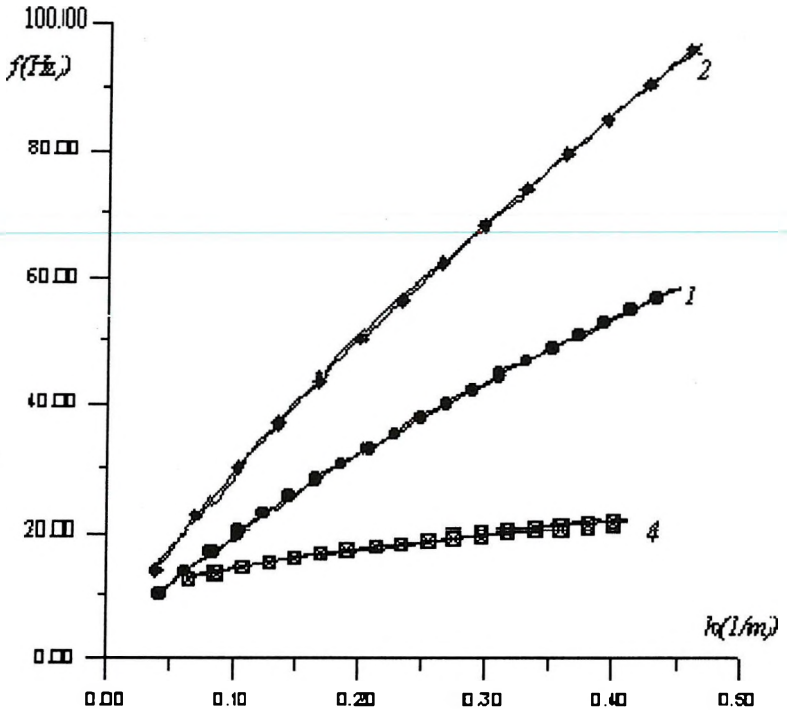

Fig. 2. Selected events from *f-k* diagram of the seismogram in Fig. 1
2. ábra. Az 1. ábra szeizmogram egyes jelenségeinek *f-k* diagramja

For determining the actual value of parameters at the sites examined we used the fitting of the calculated and the measured dispersion curves. The goodness of fit can be measured by the relative differences:

$$\Delta a = \sqrt{\frac{1}{n}\,\Sigma\left(\frac{c_m(f)-c_c(f)}{c_m(f)}\right)^2} \tag{6}$$

where n is the number of *data*, $c_m(f)$ and $c_c(f)$ are the measured and the calculated phase velocities at frequency f.

4. Dispersion calculation

Our N-layers dispersion calculations are based on the well-known algorithm of HASKELL [1953]. In this formulation the phase velocity curves can be determined by the (c, f) root pairs of

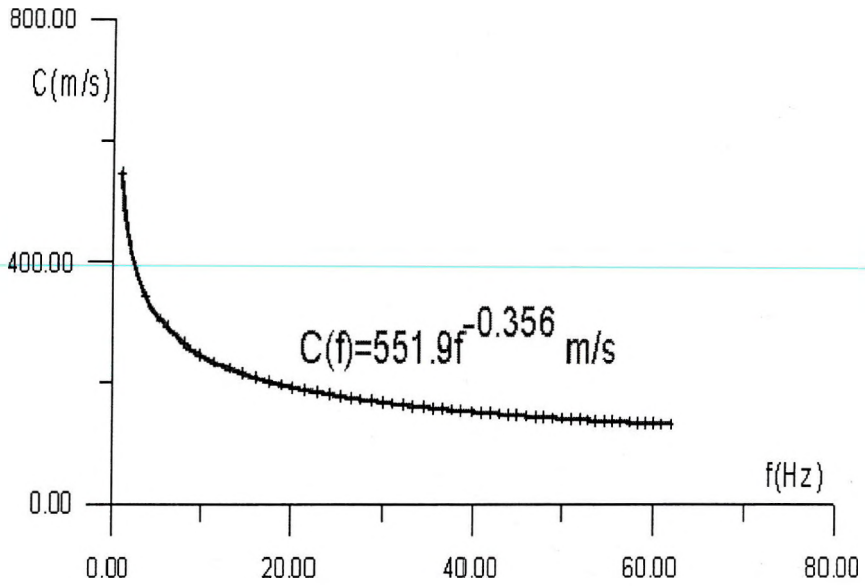

Fig. 3. C (f) phase velocity diagram of one *f–k* curve of Fig. 2.
3. ábra. Az egyik *f-k* diagramból számolt *C(f)* fázissebesség menet

$$F\,(c,\,f) = 0$$

where F is a relatively complex function constructed from the 4x4 layer matrices. Their elements are built from layer parameters.

Having fixed the frequency, the series of c roots give the phase velocities of fundamental and higher modes. Repeating the process at all frequencies of c_m data all c_c values can be determined.

Suitable approximation of continuous depth functions by a layered structure needs some consideration. In the case of N layers the depths of the lower- and uppermost layer interfaces (h_1, h_N) are determined by the extreme wavelengths of the dispersion data:

$$0.5\ \Lambda_{min} < h_1 < \Lambda_{min} \tag{7}$$

$$\Lambda_{max} < h_N < 2\ \Lambda_{max} \tag{8}$$

where Λ_{min} and Λ_{max} are the wavelengths of the examined dispersion data.

For the intermediate layers the ratio of layer thickness d_i to the layer depths h_{mi}, i.e. the value of

$$R = d_i / h_{mi}\ , \tag{9}$$

must be between 0.2 and 0.3, where

$$d_i=(h_i - h_{i-1}). \tag{10}$$

and the layer depth is defined as

$$h_{mi} = (h_{i-1}+h_i)/2 . \tag{11}$$

From these

$$h_i = h_{i-1}\ q \tag{12}$$

where

$$q = (R+2)/(2-R) \tag{13}$$

Using relations (7)–(11) the number of layers can be estimated as:

$$N= 5 + 10 \log (\Lambda_{max}/\Lambda_{min}).$$

In our practice the value of N is usually between 12 and 30.

The seismic parameter of layer i can be set by minimizing

$$\int_{h_{i-1}}^{h_i}(P(z) - P_i)^2 \, dz$$

5. Results of fitting

As mentioned above by preliminary investigations for the velocity–depth relationship the function of type (2) proved to be the best. The results of the fitting procedure can be seen in *Fig. 4a*.

Here we give the velocity and density parameters of the best fitting function for the 1st layer, (index $S1$ for transversal, index $P1$ for longitudinal) above the level of water saturation (down to 30 m)

A_{S1}=150 1 /s
n_{S1} = 3.55
A_{P1} = 300 1/s
n_{P1} = 3.65
ρ_k = 1.7 10^3 kg/m^3
ρ_v = 2.0 10^3 kg/m^3
K_1=0.12 1/m;

the parameters below 30 m are: V_S=420 m/s, V_P=1600 m/s, ρ=2.3 10^3 kg/m^3.

6. Global sensitivity

During the fitting procedure we might have got data for the sensitivity of approximation of the various type of parameters. Below, we list the ratio of

relative deterioration (increase) of Δa caused by the 1% change of parameters around its best P_0 values:

p	$d\Delta a/\Delta a$
V_{S1}	16.6%
n_S	4.9%
V_{P1}	3.2%
n_P	1.5%
ρ_k	0.4%
ρ_v	0.04%
k	0.3%

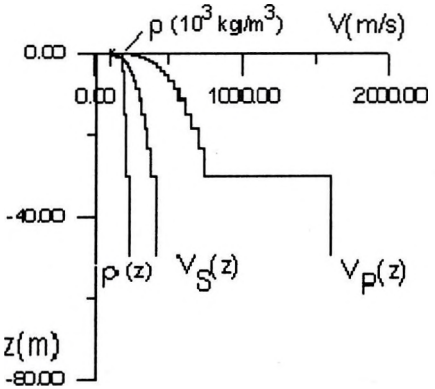

Fig. 4a. Layered model fitted to the dispersion curve
4a. ábra. A diszperziós görbéhez illesztett rétegmodell

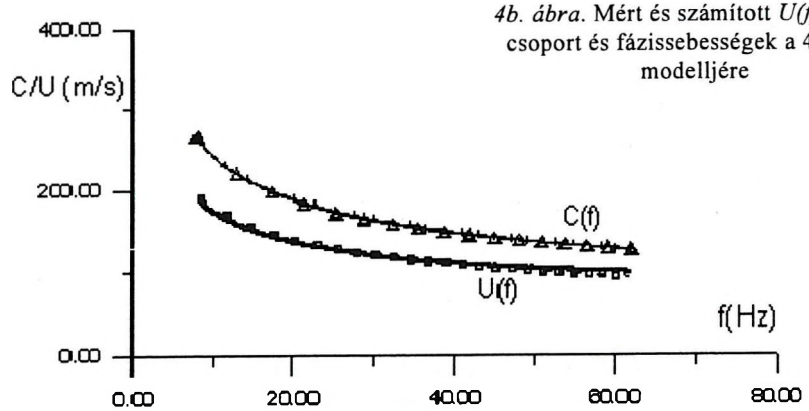

Fig. 4b. Measured and computed phase $C(f)$ and group $U(f)$ velocity for the model of Fig. 4a
4b. ábra. Mért és számított $U(f)$ és $C(f)$ csoport és fázissebességek a 4a. ábra modelljére

i.e. the variation caused by a change in V_{S1} — for example — is fivefold that of the variation caused by the same relative change in V_{P1}.

These data are in accordance with the well-known fact that the dispersion curves are governed mainly by the *S*-velocity structure of the medium.

7. Investigation of differential sensitivity

Using the layered models described above it is easy to investigate the perturbations of dispersion curves caused by the alteration of seismic parameters of a single layer. Examination of these functions can provide insight into the contribution of the different seismic parameters at different depths to the structure of the *c(f)* function [NATAF et al. 1986]. In this investigation we have used a smooth model having 32 layers.

For a layer at an intermediate depth the perturbations belonging to the different relative changes of the V_S, V_P and ρ are shown in *Fig. 5*. It can be seen that this relatively thin layer (R=0.2) has a broad-band effect on the dispersion curve. On the curves — at least in the cases of small perturbations — well defined f_π 'peak frequencies' can be seen and using the equation

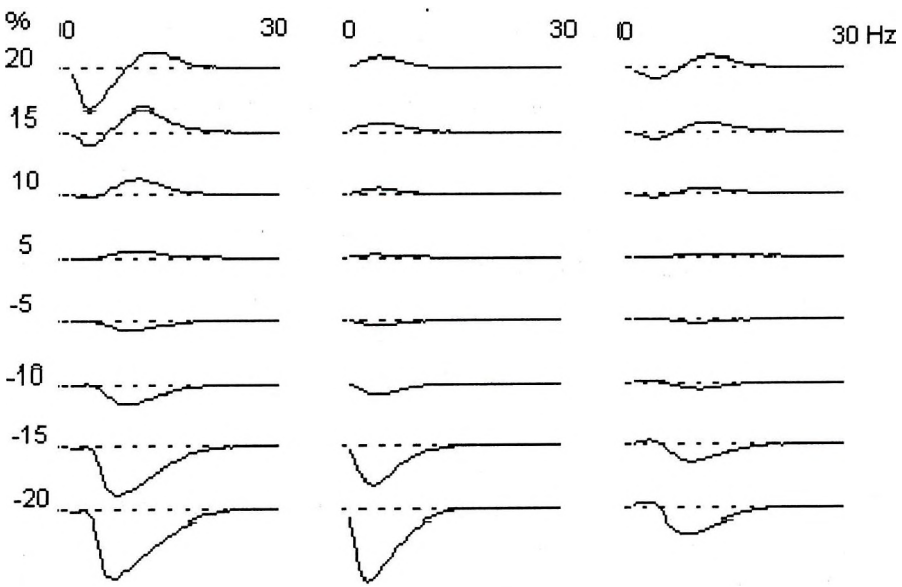

Fig. 5. Changes in the dispersion curve caused by the modification of layer parameters (V_P, V_S and ρ)

5. ábra. A diszperziós görbe megváltozása a rétegparaméterek (V_P, V_S, ρ) módosításának hatására

$$\Lambda_\pi = c_0 (f_\pi)/f_\pi$$

'peak wavelength' can be calculated (here $c_0(f)$ is the nonperturbed dispersion curve). Taking the depth of the modified layer as 'peak wavelength-layer depth' (see equation (11)) it is found that there is a linear relationship between them, i.e. $\Lambda_\pi = a \cdot h_m$ (*Fig. 6*).

Because of the significant width of the perturbation functions (Fig. 5) the phase velocity determined at one frequency involves not only one layer but the neighbouring ones, too. Their influence decreases with the increasing 'distance' of the neighbouring layers. The half-peak interval of this effect — which is the depth resolution of the fitting or, generally speaking the inversion — has been found to be linear $W = b \cdot h_m$, too (Fig. 6).

By regression we obtained different values of a and b parameters for *P*- and *SV*-waves

$$a_P = 6.04 \qquad b_P = 1.86 \text{ for } P\text{-waves}$$

and

$$a_S = 2.17 \qquad b_S = 0.91 \text{ for } S\text{-waves.}$$

The value of $a_S = 2.17$ is in good agreement with the ratio

$$r = \Lambda / z$$

widely used in the simplified inversion of ground roll dispersion [MATTHEWS et al. 1996].

In this '*rule of thumb' inversion the* $V_S(z)$ profile is approximated from the measured dispersion data simply by

$$V_S(z) = 1.1\, c_m(\lambda_m = r\, z), \tag{14}$$

where $\lambda_m = c_m/f_m$ and the value of r is between 2 and 4.

Using formulae (2), (4) and (14) the relation of parameters of $C(f)$ and $V_S(z)$ can be determined from the following equations:

$$V_S(z) = Az^{1/n} = 1.1\, c_1^{(1/(m+1))} r^{(m/(m+1))} z^{(m/(m+1))} \text{ (m/s)}$$

$$A = 1.1\, c_1^{(1/(m+1))} r^{(m/(m+1))} \text{ (1/s)}$$

and

$$n = (m+1)/m$$

i.e. the initial parameters of the $V_S(z)$ function for the fitting can be estimated from the measured dispersion data.

With the values of $c_1 = 552$, $m = 0.355$ (Fig. 3) and $r = 2.17$ we have

$$n_S = 3.81 \quad \text{and} \quad A = 143 \text{ /s}$$

in good agreement with the data of final fitting (Fig. 4)

$$n_S = 3.55 \quad A = V_{S1} = 150 \text{ /s}$$

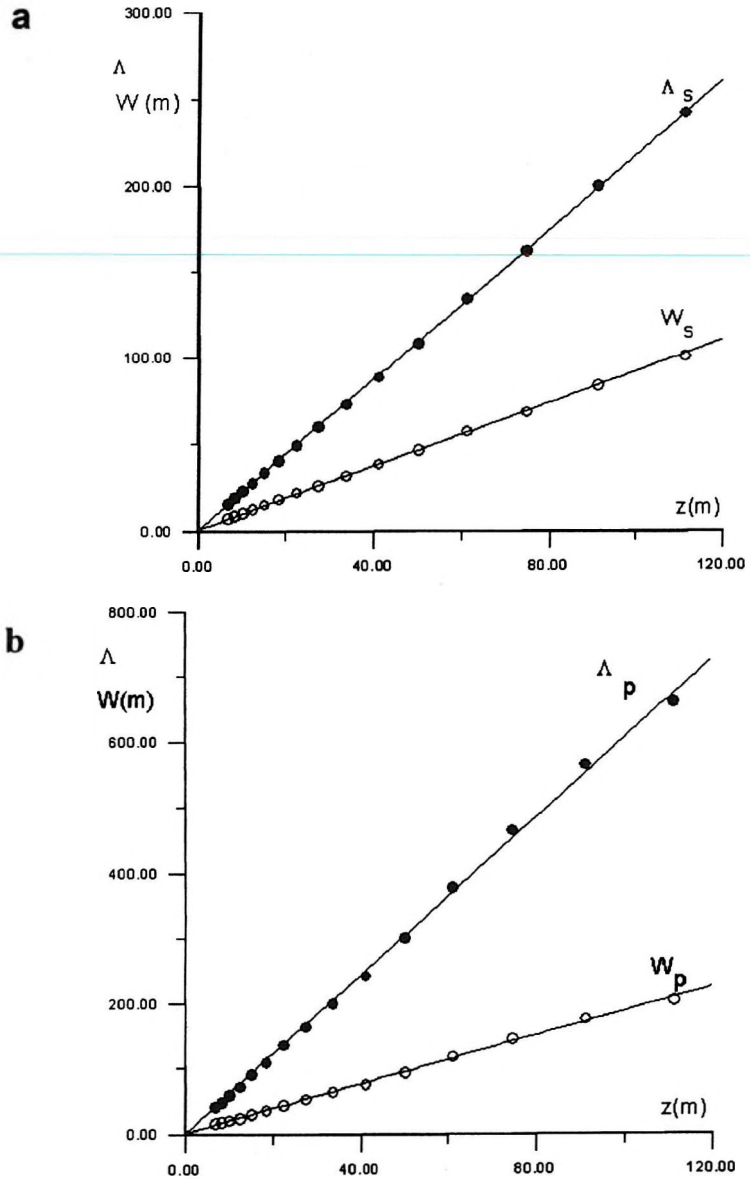

Fig. 6. Relation between the layer-depth and the perturbation parameters **a)** for *SV*-waves and **b)** for *P*-waves

6. ábra. A rétegmélység és a perturbációs paraméterek kapcsolata **a)** az *SV*-, **b)** a *P*-hullámra

8. Conclusions

Ground roll is a somewhat complicated and not very definite phenomenon in seismic prospecting. It differs from the direct or refracted first break arrivals because it has *a well defined apparent velocity change (diving wave) and dispersion* characteristics due to the very loose character of sediments. The approximation of depth dependent seismic parameters by simple analytical functions can be a useful tool in analysing ground roll dispersion caused by the inhomogeneous nature of loose sediments.

Acknowledgement

The authors thank the Hungarian Science Foundation for the grant (No.T015850.) covering the project and we are grateful to our colleagues of the Geophysical Research Division of ELGI for field work.

LITERATURE

AL-CHALABI M. 1997: Time–depth relationships for multi-layer depth conversion. Geophysical Prospecting **45**, 4, pp. 715–721

ANSTEY N. A. 1986: Whatever happened to ground roll? Geophysics: The leading edge of exploration **5**, 3, pp. 40–46 Part 1.

ÁDÁM O. 1954: The reasons for the NR (no-reflection) nature of some areas in SW Transdanubia. (in Hungarian) Geofizikai Közlemények **IV**, 1, pp. 3–10

ÁDÁM O., Sz. KILÉNYI É. 1963: Approximate velocity function from refraction travel time diagrams. (in Hungarian) Geofizikai Közlemények **XIII**, 1, pp. 61–70

ÁDÁM O. 1964: A dynamic test of ground roll. (in Hungarian) Magyar Geofizika **V**, 1–2, pp. 39–50

ÁDÁM O. 1969: Analysis of the seismic ground roll. Acta Geodet., Geophs. et Montanist. Acad.Sci.Hung. **4**, 1–2, pp. 95–133

BANTA H. E. 1941: A refraction theory adaptable to seismic weathering problems. Geophysics **6**, 3, pp. 245–250

DOBRIN M. B. 1951: Dispersion in seismic surface waves. Geophysics **16**, 1, pp. 63–80

GABRIELS P., SNIDER R., NOLET G. 1987: In situ measurement of shear wave velocity with higher mode Rayleigh waves. Geophysical Prospecting **35**, 2, pp. 187–196

HASKELL, N. A. 1953: The dispersion of surface waves on multilayered media. BSSA **43**, pp. 17–34

KAUFMAN H. 1953: Velocity functions in seismic prospecting. Geophysics **18**, 2, pp. 289–298

KRAGH E., PEARDON L. 1995: Ground roll and polarization. First Break **13**, 9, pp. 369–378

MATTHEWS M. C., HOPE V. S., CLAYTON I. R. 1996: The use of surface waves in the determination of ground stiffness profiles. Proc.Instn,Civ Engrs Geotech . Endng. **119**. Apr. pp. 84–95

NATAF H-C., NAKANISHI I., ANDERSON D. L. 1986: Measurements of mantle wave velocities and inversion for lateral heterogeneities and anisotropy. J.G.R. **91**, B7, pp. 7261–7307

RICKER N. 1953: The form and laws of propagation of seismic wavelets. Geophysics 18, 1, pp. 10–40

SZÉNÁS Gy., ÁDÁM O. 1953: The seismological build of SW Transdanubia (in Hungarian) Geophysical Transactions **II**, 9, pp. 1–15

SCHNEIDER Ch., DRESEN L. 1994: Oberflächenwellendaten zur Lokalisierung von Altasten: ein Feldfall. Geophysical Transactions **39**, 4, pp. 233–253

TOLSTOY J., USDIN I. 1953: Dispersive properties of stratified elastic and liquid media:a ray theory. Geophysics **18**, 4, p. 844

WHITE J. E., SENGBUSH R. L. 1963: Shear waves from explosive sources. Geophysics 28, pp. 1001–1019

A zavarhullámok diszperziójának analizise analitikai sebességfüggvények esetén

ÁDÁM Oszkár és HERMANN László

A szeizmikus felszíni zavarhullámok laza — főként lösz és harmadkori — üledékekben jönnek létre, amelyekben a $V(z)$ vertikális sebességeloszlás analítikus függvényekkel is jól közelíthető. Ezek a képződmények többnyire a viszko-elasztikus kőzetmodell megjelenítőiként is felfoghatók, ha szeizmikus abszorpció és diszperzió jelensége is létezik. Ezek létezését kísérleti méréseink eredményeinek analízisével és modellezéssel kívánjuk igazolni.

ABOUT THE AUTHORS

Oszkár Ádám for a photogprah and biography, see this issue, p. 18

László Hermann received his BS (physics) in 1971 from the Eötvös Loránd University of Sciences, Budapest. Since 1976 he has been working at ELGI. His research interests are the methods of determining seismic velocities (tomography, crosshole/downhole, inversion of ground roll) and the relationships of velocities and engineering parameters of media. He is a member of the EEGS and the Association of Hungarian Geophysicists

GEOPHYSICAL TRANSACTIONS 2000
Vol. 43. Number 1. pp. 33 – 45

Near-surface resolution power of the Schlumberger sounding method: examples from Lake Fertő (Neusiedlersee) region, Austria-Hungary

Franz KOHLBECK[*], László SZARKA[**,***], Alina JELINOWSKA[***], Michel MENVIELLE[***,****], Jean-Jacques SCHOTT[+], Piotr TUCHOLKA[***], Viktor WESZTERGOM[**]

The near-surface layer-resolution power of geoelectric soundings is illustrated by means of direct comparison between the geoelectric and the core sample results. Three one-dimensional inversion techniques (classical least-squares interpretation, the Zohdy technique, and the stochastic Bayesian method) are used. All of them show more similarity with the measured core sample physical parameters (core resistivity, humidity and susceptibility) than with the drillhole lithology itself. Local inhomogeneities and very thin layers cannot be seen from the surface; in contrast, the robust layer boundaries and continuously changing layer transitions can be resolved by various geoelectric inversion methods.

Keywords: geoelectric sounding, inversion, near-surface, Neusiedlersee, Austria, Hungary

1. Introduction

The Schlumberger sounding technique (also known as 'vertical electrical sounding'), as all surface geophysical techniques, allows non-invasive insight into the electrical structure of the subsurface. In spite of its widespread application and of the increasing interest in the reliable imaging of near-surface geological structures, information about its performance for investigating very near-surface structure is very limited.

Such information can only be obtained by direct comparison of measurements of the actual resistivity profile with that obtained through inversion of the Schlumberger sounding curves. In the framework of French-Austrian and

* Technical University of Vienna, Department of Geophysics, Austria
** Geodetic and Geophysical Research Institute of the Hungarian Academy of Sciences, H-9401 Sopron, Csatkai E. u. 6-8, Hungary
*** Université Paris-Sud, CNRS-ERS 388, Orsay, France
**** Centre d'Etude des Environnements Terrestres et Planetaires, CNRS/UVSQ, Saint Maur, France
+ Ecole et Observatoire de Physique du Globe de Strasbourg, France

Manuscript received: April 14, 1999

French-Hungarian cooperations, geophysical measurements, including very precise Schlumberger soundings, were carried out in 1997 in the region of Lake Fertő (Neusiedlersee). (For earlier geophysical studies of the region see KOHLBECK et al. [1993] and [1994].) As a part of this investigation, several shallow drillholes were deepened both in Austria and in Hungary. Continuous core sampling was carried out at each site, and Schlumberger soundings were performed at the core location along different (usually two perpendicular) directions.

In this paper the resolution power of near-surface Schlumberger sounding, utilizing the highest available precision in the field is discussed. The results obtained from different inversion techniques are directly compared with the subsurface rock physical properties. A summary is given of the techniques used and here we present the results for three sites, viz. Fertőújlak, Király-tó and Lébény. A detailed analysis of laboratory data together with the near-surface geology of the region is given elsewhere [JELINOWSKA et al. 2000].

2. Description of the techniques

Schlumberger sounding

With the advent of technological and computational development the resolution power of the Schlumberger sounding method (for a full description, see KOEFOED [1979]) has been significantly improved. Nowadays the main limitation of the method is the time requirement to implant the electrodes into the soil, with minimum geometrical error. In order to get very precise data within minutes, a special tool was employed. A wooden rod (made up of three lengths of 2.2 m, for ease of transportation) was prepared and perforated at preselected electrode locations. (The *AB* lengths were evenly distributed on a 20 holes/decade logarithmic scale between *AB*=500 mm and 6400 mm, and holes for three different *MN* distances, *MN* =100, 200 and 500 mm, were made, too.) At larger distances, traditional cable markers were used, still with 20 *AB* distances/length decade.

Soundings were carried out at different directions. Only a small difference was observed between the sounding curves, indicating that horizontally stratified layers can be assumed. Therefore we simply took the arithmetic mean of sounding curves measured in two perpendicular directions. Such sounding curves are shown for three sites (Fertőújlak, Király-tó and Lébény) in *Figure 1*.

Inversion techniques

Geoelectric inversion is inherently ambiguous for horizontally layered problems (i.e. in one-dimensional situations). It means that an infinite set of possible horizontally layered models can give equivalent responses and these responses are the same as the field response within very small or zero errors.

We applied three different one-dimensional inversion techniques:

(1) the Zohdy method, which is an automatic linear transformation of the apparent resistivity curves into the depth–resistivity domain, based on the morphological properties of apparent resistivity sounding curves [ZOHDY 1989]. Its main limitation comes from the fact that the layer thickness is assumed to increase logarithmically with increasing depth;

(2) a least-squares inversion technique, in which a small number of homogeneous layers are considered [JOHANSSON 1975]. From such an approach we

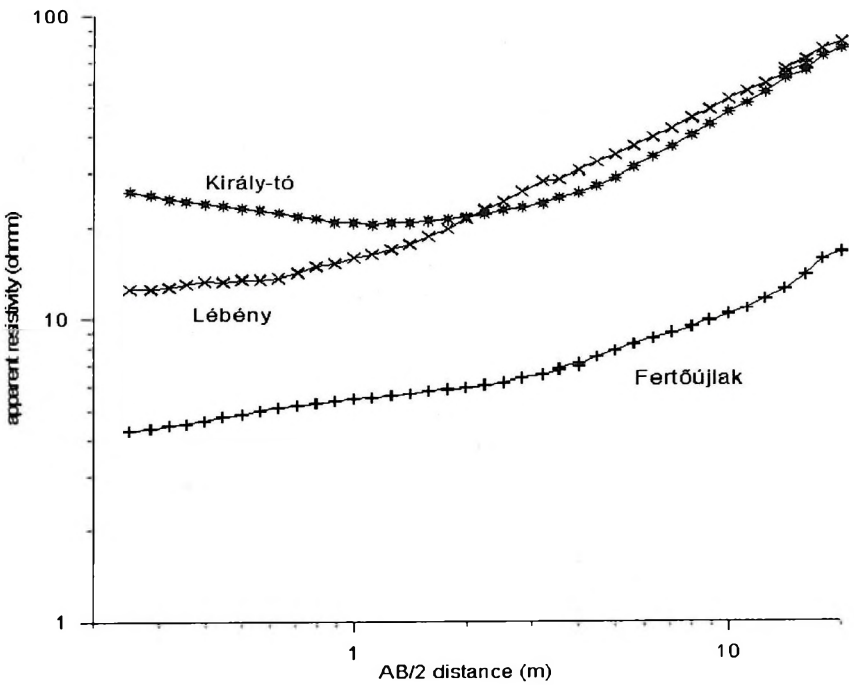

Fig. 1. Schlumberger resistivity sounding curves (mean values of two perpendicular directions, used in the geoelectric inversion) at Fertőújlak, Király-tó and Lébény

1. ábra Vertikális elektromos szondázás (azaz az inverzióhoz felhasznált, két merőleges irányban kapott szondázási görbe átlaga) Fertőújlakon, a Király-tónál és Lébény mellett

can expect that the most pronounced layers, or layer-sets, can be distinguished from each other;

(3) the stochastic Bayesian inversion elaborated by SCHOTT et al. [1999], which considers smooth models, digitized over a large number of thin layers of fixed thickness; the variable parameters are the layer resistivities. The results are the a posteriori marginal laws of the parameters over a priori preselected resistivity ranges.

Laboratory measurements on the core samples

The drillholes were deepened by using a manual drilling set. The core samples with a diameter of 5 cm were collected in about 50 cm long sections. They were immediately sealed from the air and the measurements were carried out later in the laboratory of the University of Orsay. For further investigations 22 mm x 22 mm x 22 mm standard perspex cubes were pushed into the sediment. The susceptibility and the water content were measured using standard methods; for the susceptibility a Bartington MS–2 susceptibility meter was used. The electric resistivity of core samples was measured by using a new, self-made technique (a detailed description is given in the Appendix.)

3. Results

Figures 2, 3, and *4* present observed morphological and measured physical (susceptibility, water content, and electrical resistivity) core properties for the three sites, viz. Fertőújlak, Király-tó and Lébény. Results of the inversion

Fig. 2. Lithological and physical properties of near-surface layers at the Fertőújlak site. From left to right: (a) observed lithology of the core; measured variations of physical parameters along the core: (b) susceptibility, (c) water content, and (d) electrical resistivity; resistivity profiles deduced from the inversion of the Schlumberger sounding curves given in Figure 1 using three one-dimensional inversion techniques: (e) Zohdy [ZOHDY 1989], (f) least-square fitting with a few-layers model, and (g) stochastic Bayesian method [SCHOTT et al. 1999]

2. ábra. A fertőújlaki mérési hely felszínközeli rétegeinek litológiai és fizikai tulajdonságai. Balról jobbra: (a) fúrómag litológiai szelvénye; majd a fúrómagban mért három fizikai paraméter-szelvény: (b) szuszceptibilitás, (c) víztartalom, és (d) elektromos fajlagos ellenállás; s ezután az 1. ábrán bemutatott vertikális elektromos szondázási görbékből nyert fajlagos ellenállás-mélységszelvények, három egydimenziós inverziós eljárás alkalmazásával: (e) Zohdy-eljárás [ZOHDY 1989], (f) néhány réteges modellt szolgáltató legkisebb négyzetes illesztés, és (g) sztochasztikus Bayes inverzió [SCHOTT et al. 1999]

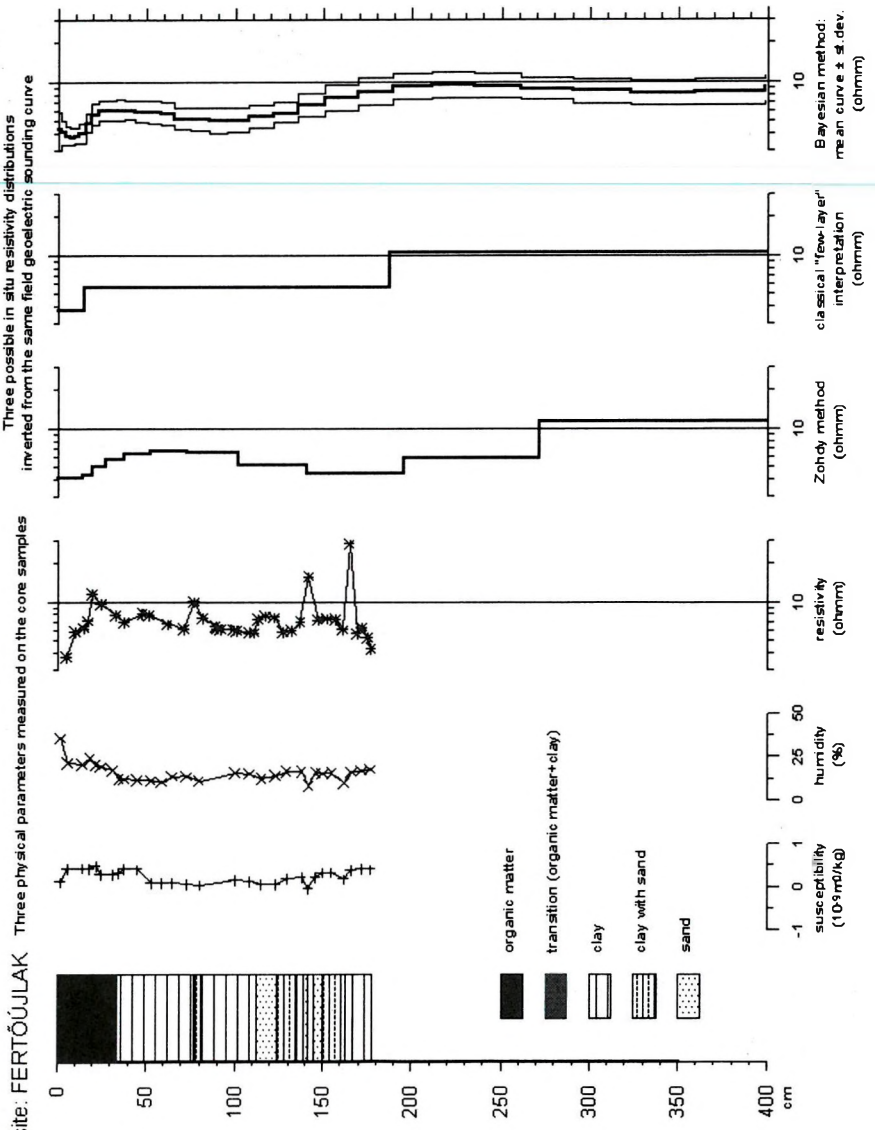
site: FERTŐÚJLAK
Three physical parameters measured on the core samples
Three possible in situ resistivity distributions inverted from the same field geoelectric sounding curve
0
50
100
150
200
250
300
350
400
cm
organic matter
transition (organic matter+clay)
clay
clay with sand
sand
susceptibility (10-3m0/kg)
-1
0
1
humidity (%)
0
25
50
resistivity (ohmm)
10
Zohdy method (ohmm)
10
classical "few-layer" interpretation (ohmm)
10
Bayesian method: mean curve ± st.dev. (ohmm)
10

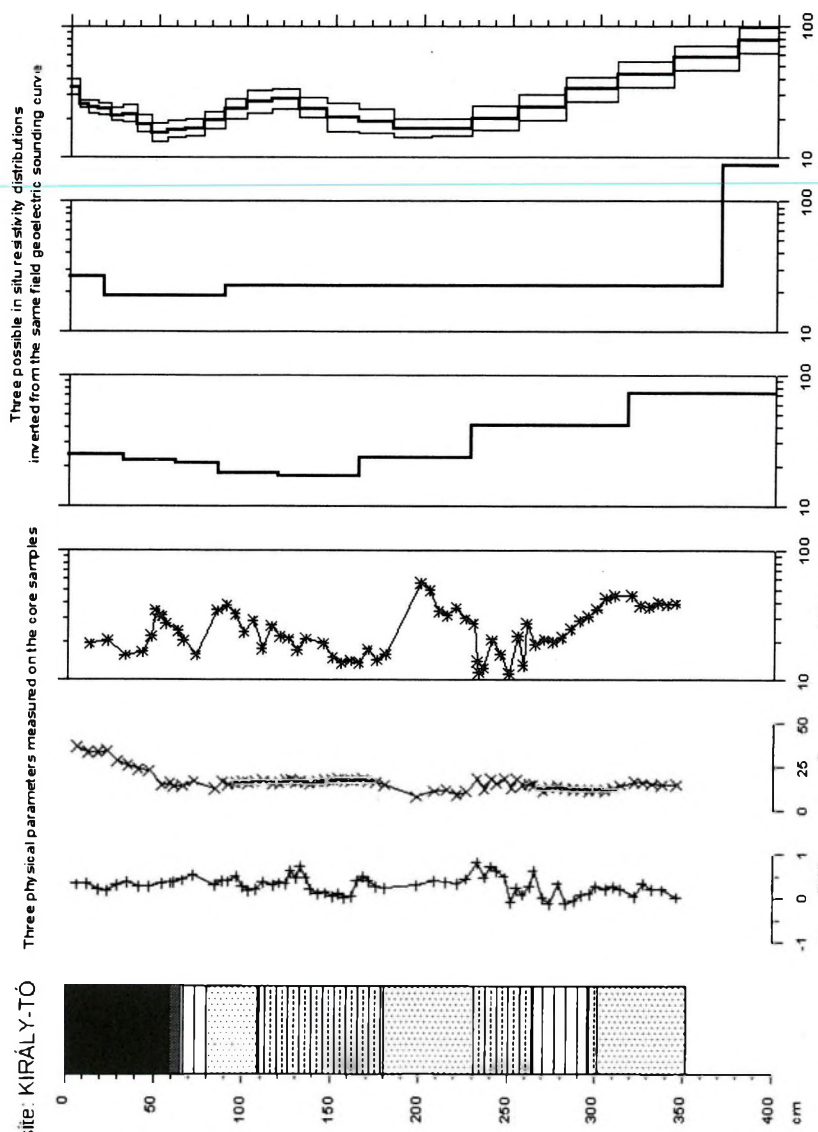

Fig. 3. Lithological and physical properties of near-surface layers at the Király-tó site (see Figure 2 for further details).

3. ábra. A Király-tavi mérési hely felszínközeli rétegeinek litológiai és fizikai tulajdonságai. (A részleteket ld. a 2. ábra aláírásában)

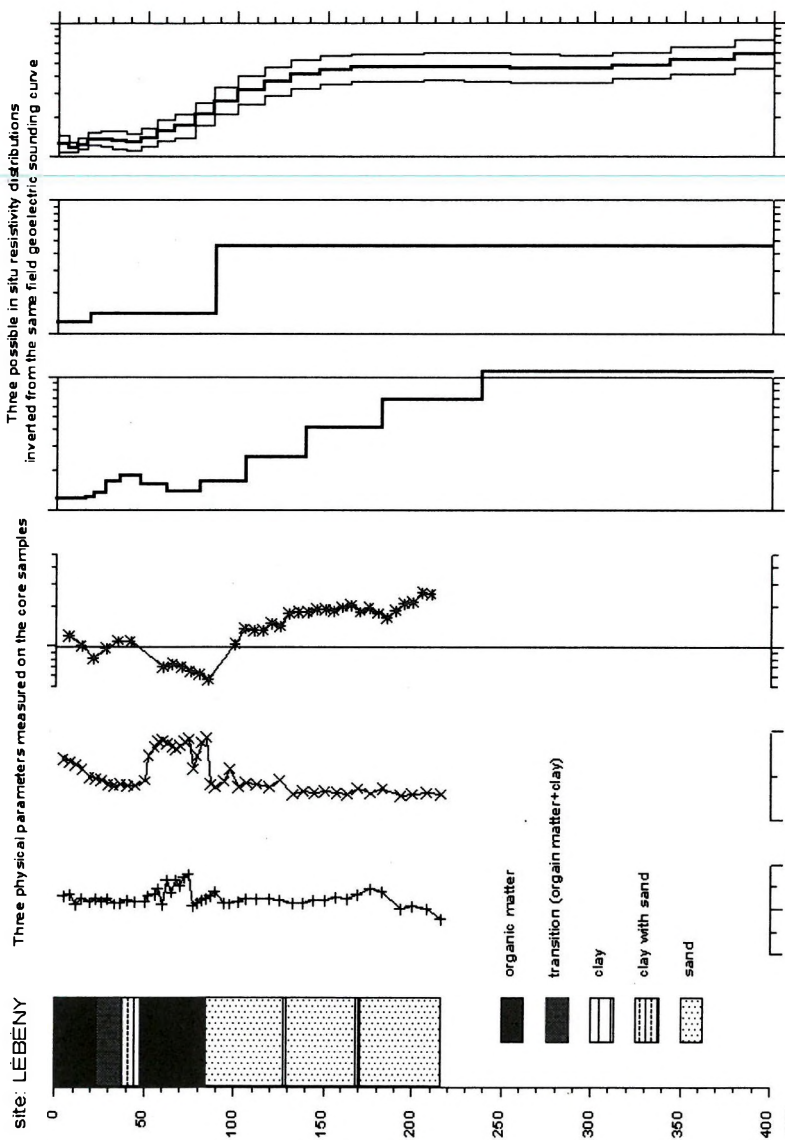

Fig. 4. Lithological and physical properties of near-surface layers at the Lébény site (see Figure 2 for further details).
4. ábra. A lébényi mérési hely felszínközeli rétegeinek litológiai és fizikai tulajdonságai. (A részleteket ld. a 2. ábra aláírásában)

of the Schlumberger sounding curves (shown in Figure 1), using the three aforementioned one-dimensional inversion techniques (Zohdy, least-squares fitting, and stochastic Bayesian methods), are also presented in these figures.

The inversion results are given to a depth of 4 m, which is greater than any of the drillhole depths. At each site, the three resistivity–depth profiles obtained are actually quite different, thereby giving a clear illustration of the non-uniqueness of the inverse problem. Their mean values are, however in good agreement with the measured core resistivity values, though all the details of the measured core resistivity profiles are not seen in the inverted profiles. This filtering out is expected either because the effect of very thin and relatively deep layers is too small to be observed, or because some changes in the core sample resistivity values might correspond to very local inhomogeneities and not to realistic layers.

For Fertőújlak the near-surface resistivity increase in the upper part of the layer of organic origin (between 0–25 cm) can be seen in all three inversion results, but the resistivity decrease observed just below it (between 25 cm and 50 cm) cannot be seen in any of them. The deeper and small resistivity changes are not detectable, either.

For Király-tó the detailed resistivity structure of the uppermost 100 cm cannot be seen from the Schlumberger sounding, though the resistivity decrease in the upper 50 cm, as well as the resistivity increase below 250 cm, is visible on all three inversion results.

For Lébény the core sample resistivity profile and the Zohdy resistivity profile run nearly parallel. A resistivity decrease between 30 and 40 cm, followed by a resistivity decrease between about 60 and 80 cm can be equally well seen. The classical inversion assuming a few layers does not allow one to detect it —, with the exception of some resistivity change at a depth of about 20 cm. The Bayesian inversion gives some weak indication about this resistivity change, but it takes place at somewhat shallower depths than where it was actually observed on the core. It is, however, worth noting that the uncertainty of the resistivity determination provided by the Bayesian inversion is of the same order as the measured resistivity variation, thus indicating that it is not possible to get clear evidence of it from inversion. At the same time, the organic matter/sand layer boundary at a depth of 85 cm can be seen perfectly in the classical interpretation. Given the already mentioned non-uniqueness of the solution of the inverse problem, this result would have been difficult to interpret in the absence of direct measurements on the core.

4. Conclusion

The results from the three sites dealt with allow one to discuss the subsurface resolution of high-precision Schlumberger soundings in conditions, in which there is no one-to-one correlation between the lithology and the physical parameters (magnetic susceptibility, water content, electric resistivity) of the core. It is evident that local resistivity heterogeneities and very thin layers cannot be resolved from the surface by using any geophysical methods. Nevertheless, significant changes in the resistivities of well-developed layers, or even progressive resistivity changes can be detected from the surface by using precise Schlumberger soundings. For the first problem (correlation of lithology and physical parameters) the classical few-layer inversion techniques are preferable whereas the latter problem (inability of geophysical methods to interpret resistivity heterogeneities) can only be resolved by inversion methods, allowing smooth layer transitions. A combination of different inversion techniques and sometimes direct comparison with measurements on the core provide a useful aid in understanding the subsurface resistivity distribution.

Acknowledgements

The authors are grateful to the directors of the Austrian and Hungarian Fertő Lake National Park for permission to carry out geophysical measurements in this area. The discussions with Tibor Cserny (Hungarian Geological Survey) are also acknowledged.

Support from two bilateral exchange programmes is acknowledged: (i) a French-Hungarian one, between the OMFB and the Ministere des Affaires Etrangéres, in the framework of the French-Hungarian intergovernmental BALATON programme of co-operation in science and technology (BALATON program N° 97052); (ii) an Austrian-French one, in the framework of the French-Austrian inter-governmental AMADEUS program of co-operation in science and technology (AMADEUS program N°97017).

Appendix
Core sample resistivity measurements

The electric measurements were carried out by using a special, small-sized, four-electrode (*AMNB*) system, connected to the field instrument and simulating a Wenner sounding on the centimetre scale. The *AM, MN*, and *NB*

distances were equal to 2 cm, and — in order to have good contact with the matrix — each of the electrodes had a length of 20 mm and a diameter of 2 mm. The $R = \Delta U/I$ electric resistance values were measured along the cores at every 5 cm, applying the smallest possible current intensity. For the computation of apparent resistivities from these resistance values, instead of a theoretical determination of geometrical coefficient for electrodes penetrating into a cylinder, a physically-based correction factor was used as follows.

In the first step of the physical correction, detailed resistance measurements were carried out with the field equipment along three parallel profiles of a more or less homogeneous core sample. The arithmetic mean of all measurements was found to be 62.3 Ωm, with a standard deviation of 1.1 Ωm. In the second step of the correction, large sheet electrodes were connected to the ends of a 26 cm long section of the same core sample, and the potential differences due to the current flowing along the core sample were measured in the central section of the sample by using different *MN* distances. The measured resistance values ($R = \Delta U / I$) were found to be proportional to the *MN* lengths, as had been expected from the following form of the differential Ohm's law: $R = \rho_c \, MN / A$, where A is the cross section of the sample. In our case A was 15.9 cm^2. The specific resistivity of the core was then directly obtained from the above equation. For the selected core sample we found $\rho_c = 6.98$ Ωm. This means that to transform all $\Delta U/I$ resistance values into resistivity values the correction factor in our case was 6.98 Ωm / 62.3 Ω = 0.112 m (within 2 % of error). In order to avoid any confusion either with results of direct resistivity measurements or with apparent resistivity ρ_{app}, this transformed resistivity ρ_c is denoted as 'core resistivity' throughout the paper.

REFERENCES

JELINOWSKA A., TUCHOLKA P., CARVALLO C., WESZTERGOM V., KOHLBECK F., MENVIELLE M., SZARKA L. 2000: Some magnetic properties of sediments from Lake Fertő (Neusiedlersee). Acta Geod. Geoph. Hung. (in print)

JOHANSSON H. K. 1975: An interactive computer/graphic-display-terminal system for interpretation of resistivity soundings. Geophysical Prospecting **23**, pp. 449–459

KOEFOED O. 1979: Geosounding principles. Volume 1 — Resistivity sounding measurements. Elsevier, Amsterdam

KOHLBECK F., SZARKA L., STEINER T., HOLLÓ L., MÜLLER I. 1993: Lake-bottom geoelectric and water-born VLF measurements on the Lake Fertő (Neusiedlersee). Paper D051, *In*: Extended Abstracts of Papers. 55th EAEG Meeting and Technical Exhibition. Stavanger, Norway — 7–11 June 1993

KOHLBECK F., SZARKA L., PÁSZTOR P., STALLBAUMER H. 1994: New geoelectric results from the Lake (Neusiedlersee). Paper P131, *In*: Extended Abstracts of Papers. 56th EAEG Meeting and Technical Exhibition, Vienna, Austria — 6–10 June 1994.

SCHOTT J. J., ROUSSIGNOL M., MENVIELLE M., RANAIVO-NOMENJANAHARY F. 1999: Bayesian inversion with Markov chains — II. The one-dimensional DC multilayer case. Geophysical Journal International **138**, pp. 769–783

ZOHDY A. A. R. 1989: A new method for the automatic interpretation of Schlumberger and Wenner sounding curves. Geophysics **54**, pp. 245–253

A vertikális elektromos szondázás felbontóképesssége felszínközeli mérések esetén

Franz KOHLBECK, SZARKA László, Alina JELINOWSKA,
Michel MENVIELLE, Jean-Jacques SCHOTT, Piotr TUCHOLKA, WESZTERGOM Viktor

Nagy geometriai pontossággal (20 adat/dekáddal; az AB=6,4 m-nél kisebb tápelektróda távolság esetén mindössze mm-nagyságú geometriai hibával) végzett vertikális elektromos szondázás felszínközeli rétegekre vonatkozó felbontóképességét a felszíni geoelektromos- és a magminta-eredmények közvetlen összehasonlításával szemléltetjük. Három különböző egydimenziós inverziós eljárást használtunk: a klasszikus legkisebb négyzetes kiegyenlítés módszerével néhány vízszintes réteget szolgáltató megoldást, a Zohdy-eljárást és a sztochasztikus Bayes-módszert. Mindhárom eljárás eredménye nagyobb hasonlóságot mutat a folyamatosan vett fúrómagon mért fizikai paraméter-szelvényekkel (az elektromos fajlagos ellenállással, a víztartalommal és a mágneses szuszceptibilitással), mint a fúrómagon szemmel megfigyelhető litológiai változásokkal. Helyi inhomogenitások és nagyon vékony rétegek a felszínről nem mutathatók ki, de a jól kifejlett réteghatárok és a rétegződés folyamatos változásai megjelennek a különböző inverziós eredményekben.

ABOUT THE AUTHORS

Franz Kohlbeck (1943, Vienna) graduated Dipl.-Ing. (physics) from the Vienna University of Technology in 1969. He was then offered a post at the Institute of Mechanical Technology and Engineering Material Sciences. At the same time he started his dissertation work at the Reaktorzentrum Seibersdorf (now: Seibersdorf research centre). In 1974 he was awarded his Ph.D. for his work on calculating cell-dimensions from d-values of powder diffraction patterns. With a view to carrying out research on rock mechanics, in 1975 he returned to the Vienna University of Technology. He was appointed docent for Engineering Geophysics in 1981. Since then, he has worked mainly on environmental geophysics, particularly on geoelectrics. On two occasions, he was an invited Professor at the National University of Bogota, Colombia. From 1991 to 1993 he headed the department of Geophysics of the Institute of Theoretical Geodesy and Geophysics; he has been professor since 1994.

László Szarka (1954, Derecske) graduated in 1977 as geophysical engineer from Miskolc University. Since that time he has carried out research work in the field of electromagnetic geophysics at the Geodetic and Geophysical Research Institute of the Hungarian Academy of Sciences, in Sopron. Currently, he is scientific adviser and head of the electromagnetic department. He became D.Sc. (earth sciences) in 1997. After a habilitation at Miskolc University, he was nominated head of the Geoscience Institute of Sopron University (now: University of Western Hungary). Between 1997 and 1999 he worked as part-time associate professor at the University of Orsay (Université Paris Sud XI).

Alina Jelinowska, geologist-geophysicist, graduated in 1985 from the University of Warsaw (Poland); she was awarded her postgraduate diploma at the University of Orsay, in 1988. Her Ph.D. thesis dealing with the magnetic properties of lake sediments as indicators of palaeoclimatic and environmental evolution in continental Quaternary sections was awarded in 1995 by the same university. She holds the title Maitre de Conferences at University of Orsay; her major research interests cover magnetic mineralogy in sediments and its relationship with environmental parameters. Recent works of hers has dealt with Caspian and Black Seas sediments and east-European Upper Quaternary sequences.

Michel Menvielle (1951, Paris) graduated as an engineer at the Ecole Centrale de Paris, France, in 1974. He joined the Institut de Physique du Globe de Paris. In 1984, his These d'Etat was awarded for his work on electromagnetic induction. He is now a professor at the University of Orsay, and belongs to the C.E.T.P. (Centre d'étude des Environnements Terrestre et Planétaires, Saint Maur, France). His work deals with the study and characterization by indices of transient magnetic activity observed at the Earth's surface, and with the application of induction methods to determining the electric structure of the solid Earth using a Bayesian approach. More generally, he is interested in using surface magnetic measurements for understanding inner and outer planetary structure and dynamics; in particular, he is involved in magnetic experiments on board Mars landers.

Jean-Jacques Schott (1947) graduated in physics in 1969. He joined the Institut de Physique du Globe de Strasbourg in 1973, where he began studies in palaeomagnetism applied to plate tectonics. He was awarded his M.Sc. in 1977, and his state qualification (1985) focused on palaeomagnetism in the Iberian plate. He then worked on modelling the apparent polar wander path using parametric and non-parametric methods. He is now assistant professor and deals with two different domains: geoelectrical subsurface imaging and geomagnetism. Since 1998, he has headed the Department of Geomagnetic Observatories at E.O.S.T., (Ecole et Observatoire des Sciences de la Terre de Strasbourg).

Piotr Tucholka graduated in 1970 at the Department of Geology, University of Warsaw (Poland), specializing in geophysical well-logging. He worked (1970–79) at the Polish Academy of Sciences in Warsaw, Poland, obtaining his Ph.D. for his work on the palaeomagnetic study of loess sequences. From 1979 to 1983 he was Leverhulme and N.E.R.C. Research Fellow at the University of Edinburgh (Scotland) where he worked on the magnetism of lake sediments and palaeosecular variation of the Earth's magnetic field. Since 1985, he has been professor at the University of Orsay, France. At present, his main research topics include palaeomagnetism and the palaeoenvironment, and the application of shallow geophysics to environmental problems.

Viktor Wesztergom (1959, Mosonmagyaróvár) studied geophysics at the Eötvös Loránd University in Budapest, graduating in 1983. From 1983 to 1986 he worked at the Eötvös Loránd Geophysical Institute. He also qualified at Budapest's University of Economics. In 1995, he was awarded his Ph.D. Since 1986 he has been at the Geodetic and Geophysical Research Institute of the Hungarian Academy of Sciences. His main research topics are the geomagnetic field of external origin and geomagnetic induction. In addition to his research work, he is the head of Geophysical Observatory István Széchenyi near Sopron and editor of Acta Geodaetica et Geophysica Hungarica.

GEOPHYSICAL TRANSACTIONS 2000
Vol. 43. Number 1. pp. 47 – 63

Quality controlled resistivity inversion in cavity detection

Zsuzsanna NYÁRI*

Cavity detection is a common problem in engineering geophysics. Resistivity methods have been widely used for such tasks since the development of multi-electrode measuring systems. These new computer controlled data collecting systems provide large amounts of data in a short time. This paper presents the latest theoretical developments of ELGI in processing geoelectric data for the use of near surface cavity detection.

When, apart from the location, the size and the depth of cavities are needed an inversion method based on 2-D analytic model calculations can be used; this method also gives their uncertainty. After numeric tests this inversion method has been successfully applied on field data.

To improve the reliability of the cavity parameters a simultaneous inversion method has been developed whose inputs are two datasets measured by different electrode arrays (dipole–dipole and Wenner) along the same profile. The results of the numeric investigations prove that this processing method gives more reliable solutions than the simple inversion method.

Keywords: resitivity, electrodes, two-dimensional models, cavity, inversion, engineering geophysics

1. Introduction

Near surface cavities mean real danger for traffic and buildings. It is a serious task for engineering geophysics to locate such cavities and it is often necessary to determine reliably their dimensions. Resistivity measurements have been more widely used for such problems since the development of multi-electrode measuring systems, which provide fast data collection.

Resistivity measurements are carried out along a profile where data measured at different electrode separations represent different depths of investigation. The result of the measurement is a 2-D pseudo-section with the raw resistivity data. These pseudo-sections can be processed by FD or FE inversion methods such as was done, for example, by DEY and MORRISON [1979]. BARKER [1992] invented a fast inversion reconstruction method based on a quasi-Newton procedure using only one iteration step. LOKE and BARKER [1996] improved this process and inserted it into an inversion algorithm. Us-

* Eötvös Loránd Geophysical Institute of Hungary, H-1145 Budapest, Kolumbusz u. 17–23
Manuscript received (revised version): 22 September, 1999.

ing FD inversion methods the geoelectric characteristics of the investigated area can be correctly mapped and the anomalies caused by cavities can be reliably marked. GYULAI [1996–1997] invented a 1.5-D FD inversion method especially for cavity detection.

An inversion method whose forward calculation is carried out using the analytic solution of the 2-D cavity model has been developed in order to give rapidly and reliably the positions and size of the investigated objects. This process provides the parameters (location, size, depth) of the cavities along the profile. It is also possible to calculate the reliability values of the model parameters.

Joint inversion uses two (or more) independent methods for measuring along the profile. If joint inversion is applied the investigated parameters can be more correctly estimated than in the case of single inversion. DOBRÓKA et al. [1991] developed a joint inversion algorithm for seismic and resistivity data in the case of layered earth investigations. A method in which the components of the inversion are two datasets measured by two different electrode configurations has a similar effect on the estimated parameters as does joint inversion. GYULAI [1998] used that so-called simultaneous inversion based on 1.5-D forward calculation for cavity detection with dipole–dipole and pole–pole data. My paper will present a simultaneous inversion method based on analytic modelling of dipole–dipole and Wenner data.

2. Data processing with inversion

The inversion algorithm applied here was based on the linearized, qualified inversion method developed by DOBRÓKA et al. [1991] using the Marquard algorithm and L_2 norm. This algorithm has been improved for the particular purpose of cavity detection using 2D analytic forward calculation.

As the first step of the inversion one has to define a model and give its initial parameters:

$$\overline{X} = (p_1, \ldots, p_n) \tag{1}$$

$\overline{X}$: vector of model parameters
p_j: model parameter
n: number of model parameters

In the test the 2-D geological model was a horizontal, infinite length cylinder with infinite resistivity laid in uniform halfspace (*Fig. 1*). The parameters of the model are: resistivity of the earth (ρ_1), location of the cavity along

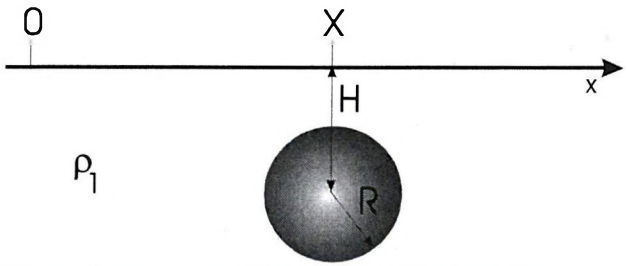

Fig. 1. The 2-D geological model for the inversion
1. ábra. 2-D geológiai modell az inverzió céljára

the profile (x), depth of the midpoint of the cylinder (H), radius of the cylinder (R). In the case of more cavities along the profile the number of parameters will increase by three times the cavity number. Forward calculation is carried out using the parameter vector defined in (1) and the $\bar{s}$ vector of the measured data:

$$Y_i^{cal} = Y(\bar{X}, s_i) \tag{2}$$

$i = 1,2,..,m$
m: number of measured data
s_i: i^{th} measured value
Y: response function

When function Y is the non-linear function of the parameter vector a linearization process is conventional. The first order Taylor expansion of Y is given by:

$$Y_i^{calc} = Y_i^0 + \sum_{j=1}^{n} \left(\frac{\partial Y_i^{calc}}{\partial x_j} \right)_{\bar{X}=\bar{X}_0} \delta x_j \tag{3}$$

$\bar{X}_0$: vector of initial model parameters
$Y_i^{(0)}=Y(X_0,s_i)$

The error vector $\bar{e}$ gives the difference between the response functions of the observed and the calculated data:

$$\bar{e} = \bar{y} - \underline{\underline{G}}\bar{x} \tag{4}$$

where:

$$y_i = \frac{Y_i^{obs} - Y_i^0}{Y_i^{obs}} \qquad x_j = \frac{\delta X_j}{X_j^0} \qquad G_{ij} = \frac{X_j^0}{Y_i^{calc}} \left(\frac{\partial Y_i^{calc}}{\partial X_j} \right)_{\bar{X}=\bar{X}_0}$$

Minimizing the error vector according to L_2 norm leads to a linear equation system:

$$\underline{\underline{G}}^T \underline{\underline{G}} \bar{x} = \underline{\underline{G}}^T \bar{y} \tag{5}$$

The Marquard-Levenberg solution of (5) is:

$$\bar{x} = \left(\underline{\underline{G}}^T \underline{\underline{G}} + \lambda I\right)^{-1} \underline{\underline{G}} \bar{y} \tag{6}$$

I: unit matrix

λ: damping factor

To decrease the errors of linearization several iteration steps are needed.

Forward calculation

The potentials of the uniform halfspace (7) and the 2D cylinder (8) with infinite length and resistivity for infinite length line electrodes were calculated by LÖSCH et al. [1979].

$$V_0(C, P_{11}, ..., P_{1q}, P_{21}, ..., P_{2q}) = \\ = \frac{I \cdot \rho_1}{\pi q}\left(\ln\frac{1}{\bar{R}_{11}} + ... + \ln\frac{1}{\bar{R}_{1q}} - \ln\frac{1}{\bar{R}_{21}} - ... - \ln\frac{1}{\bar{R}_{2q}}\right) \tag{7}$$

V_0: potential of uniform halfspace
I: current/length
C: position of current electrode
P: position of potential electrode
$\bar{R}_{rq}$: distance of current C and potential electrodes P_{rq}
r=1: positive electrode (subscript)
r=2: negative electrode (subscript)
q: number of electrode pairs (subscript)

$$V_c(\xi, \eta) = \sum_{m=1}^{\infty}\left(A_m^{(1)} \cos m\xi + B_m^{(1)} \sin\xi\right)\left(e^{m\eta} + e^{m\eta_0}\right) \tag{8}$$

V_c: potential of the cylinder
ξ, η: bipolar co-ordinates after LÖSCH et al. [1979]
A, B: integration constants

LÖSCH et al. [1979] proved by model measurements that if one applies line electrodes in a 2-D medium it results in quantitatively the same apparent resistivity values as point electrodes used in a 3-D medium. Appendix A pre-

sents some results of numeric investigations proving that the error caused by line electrodes in 2-D model calculations is smaller than 1%.

FERENCZY [1980] calculated the potentials of (7) and (8) for the case of dipole–dipole array with the assumptions that the electrodes are placed on the surface and the profile is perpendicular to the axis of the cylinder. Then the bipolar co-ordinates can be written as

$$\eta = 0 \tag{9}$$

$$\eta_0 = \ln\left(\frac{H}{R} + \sqrt{\frac{H^2}{R^2} - 1}\right) \tag{10}$$

$$\xi_q = 2\arctan\frac{\sqrt{H^2 - R^2}}{x_q} \tag{11}$$

x_q: co-ordinate of the q^{th} electrode along the profile
H, R: parameters of the 2-D model

Then the potentials in (7) and (8) for any arrays consisting of two current and two potential electrodes can be calculated as:

$$\Delta V_0 = \frac{I\rho_1}{2\pi}\left(\ln\frac{1-\cos\left(\xi_{P_1} - \xi_{C_2}\right)}{1-\cos\left(\xi_{P_1} - \xi_{C_1}\right)} - \ln\frac{1-\cos\left(\xi_{P_1} - \xi_{C_2}\right)}{1-\cos\left(\xi_{P_2} - \xi_{C_1}\right)}\right) \tag{12}$$

$$\begin{aligned}\Delta V_c = \sum_{m=1}^{\infty} \frac{2I\rho_1}{m\pi} \cdot \frac{\alpha}{e^{2m\eta_0} - \alpha} \cdot \\ \cdot \left\{\left(\cos m\xi_{C_1} - \cos m\xi_{C_2}\right)\cdot\left(\cos m\xi_{P_1} - \cos m\xi_{P_2}\right) + \right. \\ \left. + \left(\sin m\xi_{C_1} - \sin m\xi_{C_2}\right)\cdot\left(\sin m\xi_{P_1} - \sin m\xi_{P_2}\right)\right\}\end{aligned} \tag{13}$$

ρ_1: resistivity of the halfspace
ρ_2: resistivity of the cylinder

$$\alpha = \frac{\rho_2 - \rho_1}{\rho_2 + \rho_1}$$

The calculated resistivity curve of the 2-D model on *Fig. 1* can be determined from:

$$\frac{\rho_a}{\rho_1} = 1 + \frac{\Delta V_c}{\Delta V_0} \tag{14}$$

For models with more than one cavity the potential of the model can be calculated from the superposition of the anomalies of each cylinder (15), and the model resistivity can be written as (16):

$$\Delta V_s = \sum_{i=1}^{n_c} \Delta V_c^i + (n_c - 1)\Delta V_0 \tag{15}$$

$$\frac{\rho_a}{\rho_1} = 1 + \frac{\Delta V_s}{\Delta V_0} \tag{16}$$

ΔV_s: anomaly after superposition
ΔV_c^i: anomaly of i^{th} cylinder
n_c: number of cavities

Numeric investigations also prove that the effect of more cylinders can be correctly determined by the method of superposition (even in the case of cavities relatively close to each other) when the apparent resistivity is reached from separately calculated and stacked primary (ΔV_0) and secondary (ΔV_c) potentials (Appendix B).

Sensitivity investigations proved [NYÁRI 1997] that this method is not sensitive to the resistivity value of the cavity. At relative low resistivity contrast between the earth and the cavity ($\rho_2=5\rho_1$) fulfils the model assumption of infinite cylinder resistivity. For these purposes parameter ρ_2 was kept constant during the inversion process.

Qualifying of parameters

In order to qualify the calculated model parameters we followed the definitions of SALÁT et al. [1982]. When the data are uncorrelated the distribution of the model parameters can be characterized by the covariance matrix.

$$\underline{\underline{\mathrm{cov}}} = \sigma_d^2 \left(\underline{\underline{G}}^T \underline{\underline{G}} \right)^{-1} \tag{17}$$

$$\sigma_d = \sqrt{\frac{1}{m}\sum_{i=1}^{m}\left(\frac{Y^{obs} - Y^{calc}}{Y^{calc}}\right)^2}$$

m: number of data points

The diagonal elements of the covariance matrix give the uncertainty of the model parameters (variance). The off-diagonal elements describe the correlation of the parameters (18).

$$\mathrm{corr}_{ij} = \frac{\mathrm{cov}_{ij}}{\sqrt{\mathrm{cov}_{ii}\,\mathrm{cov}_{jj}}} \tag{18}$$

corr_{ij}: correlation of i^{th} and j^{th} model parameters.

Numerical investigations

In order to test the inversion algorithm for geoelectric cavity detection synthetic data have been computed. The effect of different electrode arrays with four electrodes has also been investigated. OWEN [1983] found that dipole–dipole array is the most suitable configuration for the purpose of cavity detection. However at greater depths the separation of the dipoles is large in relation to the distance of the AB and MN electrodes so in such cases the measured data contain too high noise level. The effect of resistivity anomalies on different Wenner configurations has been observed by NYÁRI [1997] with the result that the conventional Wenner (AMNB) configuration can be used the most effectively for cavity detection. So the inversion method has been tested only with datasets of these two arrays.

Different levels of Gaussian noise have been added to the analytically calculated datasets representing low (2%) and high (5%) noise (*Figs. 2, 3*). *Table I* shows the parameters of the model used and the uncertainty of the estimation after the inversion. It can be observed that the uncertainties of resistivity and location parameters are the smallest in the case of both arrays. The errors of depth and size parameters were around the added noise level at dipole–dipole, and much higher than the noise level in the case of the Wenner array.

Field example

Near-surface cavities were detected in the village of Emőd in Hungary in 1987. The measurements were carried out by GYULAI et al. [1987]. A dipole–dipole array was applied with a = 2 m unit electrode spacing, and

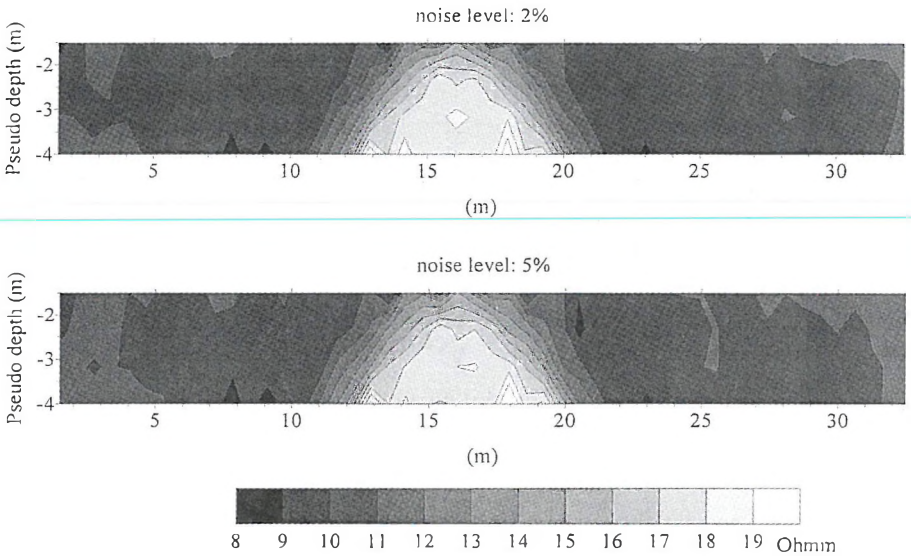

Fig. 2. Synthetic dipole–dipole pseudo sections with different noise level
2. ábra. Szintetikus dipól-dipól pszeudo szelvények különböző zajszintekkel

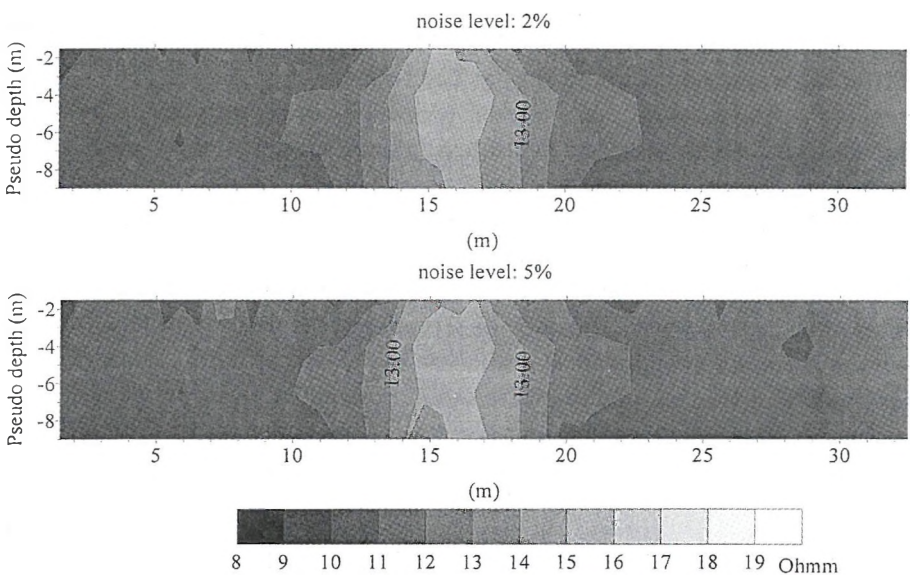

Fig. 3. Synthetic Wenner pseudo sections with different noise level
3. ábra. Szintetikus Wenner-pszeudo szelvények különböző zajszintekkel

Parameter	Uncertainties of parameters (%)			
	DD 2%	W 2%	DD 5%	W 5%
ρ_1=10 Ωm	0.34	0.59	0.48	0.8
H=3 m	3.05	7.54	4.39	10.84
R= 2 m	5.11	17.23	7.23	24.89
X=16 m	0.16	0.39	0.24	0.57

Table 1. Model parameters and their uncertainties after single inversion of datasets with different noise and electrode array. *DD n*%: dipole–dipole data with *n*% of noise level; *W n*%: Wenner data with *n*% of noise level

I. táblázat. Modellparaméterek és bizonytalansági értékeik egyszeres inverzió után különböző zajszint és elektróda elrendezés esetén. *DD n*%: dipól-dipól adatok *n*% zajszint mellett; *W n*%: Wenner adatok *n*% zajszint mellett

n = 1,2,...,5 depth levels were investigated. *Figure 4* shows the measured data. The result of the inversion is presented in *Table II.* It is interesting that the uncertainties of parameters *H* and *R* are smaller than the fitting error (13.8 %) of the measured and the calculated datasets.

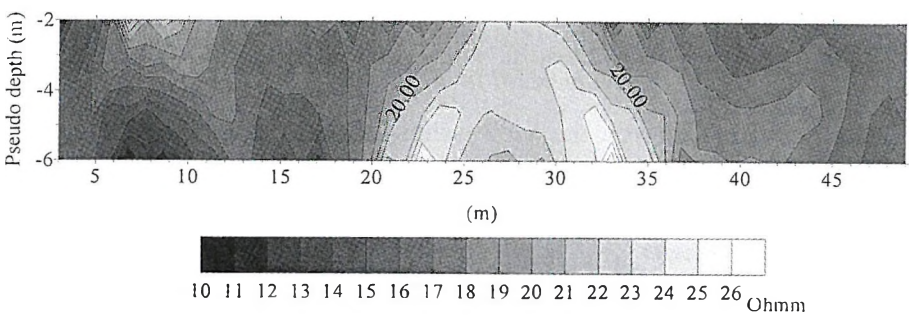

Fig. 4. Resistivity profile measured at Emőd

4. ábra. Emődnél mért ellenállászelvény

Parameters	$\tilde{n}_1$	*H*	*R*	*X*
Inverted values	16.8 Ωm	3.6 m	2.2 m	28.1 m
Uncertainties	1%	8%	8%	0%

Table II. Inversion result of resistivity profile measured at Emőd. Fitting error: 13.8%

II. táblázat. Az Emőd mellett mért ellenállásszelvény inverziós eredménye

3. Data processing with simultaneous inversion

The algorithm of simultaneous inversion is quite similar to simple inversion. The main difference is that the $\bar{s}$ vector of the measured data has two different parts depending on the arrays applied in the measurement:

$$\bar{s} = \bar{s}_1 + \bar{s}_2 \tag{19}$$

$\bar{s}_1$: vector of data measured with the first array

$\bar{s}_2$: vector of data measured with the second array.

GYULAI [1998] investigated the parameter sensitivities of some arrays. He observed that the sensitivity of geometric parameters (length, width, depth) does not change equally with different arrays. This means that one array is more sensitive for width, the other for length, etc. So if one applies two different arrays in one inversion process the whole dataset will be sensitive to both parameters.

The dipole–dipole array has almost the best horizontal resolution among the electrode configurations. However it can be applied only for detecting a small depth range because of the high noise level caused by the separation rate of the electrodes. With a Wenner array one can investigate a larger depth scale but with worse horizontal resolution. It is assumed that if one uses these two arrays together in inversion processing the uncertainties of the inverted parameters can be decreased.

Numerical investigations

The synthetic data were the same as those used in testing the simple inversion method. *Table III.* shows the errors of the model parameters of *Table I* af-

Parameter	Uncertainties of parameters (%)		
	DD 2%, W 2%	DD 5%, W 5%	DD 5%, W 2%
ρ_1=10 Ωm	0.28	0.40	0.35
H=3 m	2.39	3.42	2.97
R= 2 m	4.36	6.2	5.38
X=16 m	0.15	0.22	0.19

Table III. Model parameters and their uncertainties after simultaneous inversion of datasets with different noise and electrode array. *DDn*%: dipole–dipole data with *n*% of noise level; *Wn*%: Wenner data with *n*% of noise level

III. táblázat. Modellpraraméterek és bizonytalansági értékeik az adatok szimultán inverziója után különböző zajszintek és elektróda elrendezések esetén. *DDn*%: dipól–dipól adatok *n*% zajszint mellett; *Wn*% Wenner adatok *n*% zajszint mellett

ter simultaneous inversion. It can be observed that the errors of all parameters were smaller at both noise levels than in the errors in *Table 1*.

In the next step datasets based on real field data acquisition have been computed. This means that the dipole–dipole data contained higher noise (5%), than the Wenner data (2%). The errors of the parameters after simultaneous inversion are also presented in Table III. It is remarkable that even the noisy dipole–dipole data could reduce the uncertainties of the Wenner data as well. *Figures 5* and *6* respectively present how simultaneous inversion can reduce the errors of parameters H and R.

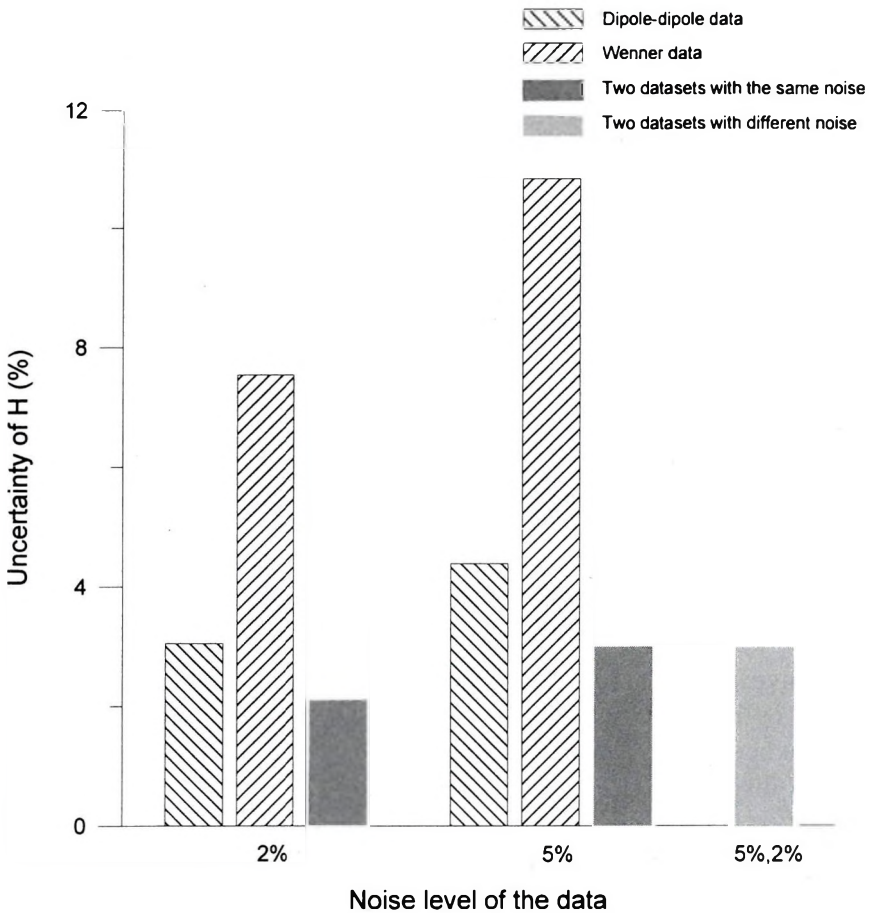

Fig. 5. Uncertainties of depth parameter after different kinds of inversions with datasets of different noise

5. ábra. A mélységparaméterek bizonytalanságai különböző inverziók után eltérő zajok mellett

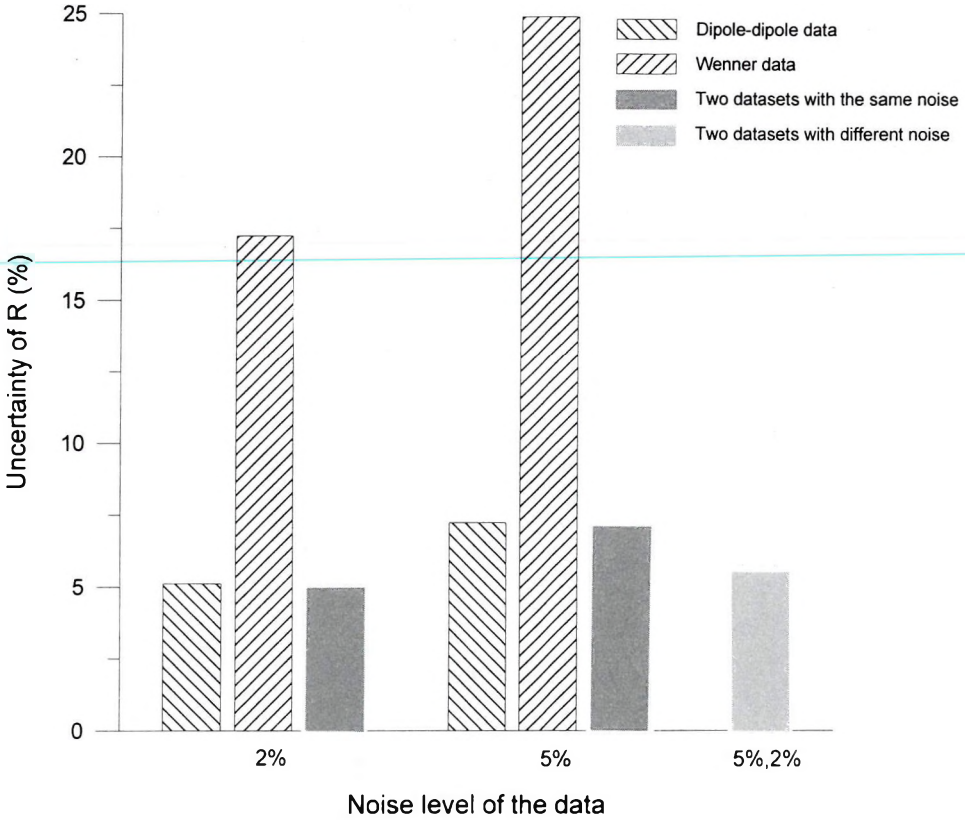

Fig. 6. Uncertainties of radius parameter after different kinds of inversions with datasets of different noise

6. ábra. A sugárparaméterek bizonytalansági értékei eltérő zajokkal terhelt adatrendszerek különböző inverziói után

To investigate the inversion method in the case of more cavities a model with two cylinders with the same *H/R* ratio (*H/R*=1.3) but different size and depth has been used. *Table IV* presents the model and qualifying parameters when the distance between the objects is relatively large. The results of the single inversion show that the reliability of the parameter estimation is better for the cylinder with shallower depth in the case of dipole–dipole, and for the cylinder with greater depth in the case of the Wenner array. If the two cylinders

V. táblázat. Modellparaméterek és bizonytalansági értékeik egyszeres és szimultán inverzió után különböző zajszintekre és eletktróda elrendezésekre egymáshoz közel lévő két henger esetén. *DD n*%: dipól-dipól adatok *n*% zajszint mellett; *W n*%: Wenner adatok *n*% zajszint mellett

Qualifying parameter	Model parameter	M1 model	DD 2%	W 2%	DD 5%	W 5%	DD 5%, W 2%
Uncertainty [%]	ρ_1	10 Ohmm	0.396	0.79	0.577	1.122	0.433
	H_1	4 m	5.198	12.97	7.625	19.58	4.747
	R_1	3 m	7.06	21.6	10.275	33.486	6.872
	X_1	10 m	0.421	1.11	0.62	1.708	0.507
	H_2	2 m	3.635	14.15	5.337	21.428	4.379
	R_2	1.5 m	6.279	27.95	9.319	44.455	7.724
	X_2	20 m	0.13	0.37	0.191	0.556	0.157
Fitting error [%]			4.21	4.33	6.131	6.173	5.393
Rel. model distance [%]			1.978	1.731	0.955	1.213	0.485
Number of data			177	147	177	147	324

Table IV. Model parameters and their uncertainties after single and simultaneous inversion of datasets with different noise and electrode array for two cylinders that are relatively far apart. *DD n*%: dipole–dipole data with *n*% of noise level; *W n*%: Wenner data with *n*% of noise level.

IV. táblázat. Modellparaméterek és bizonytalansági értékeik egyszeres és szimultán inverzió után különböző zajszintekre és eletktróda elrendezésekre egymástól viszonylag távol lévő két henger esetén. *DD n*%: dipól-dipól adatok *n*% zajszint mellett; *W n*%: Wenner adatok *n*% zajszint mellett

Qualifying parameter	Model parameter	M2 model	DD 2%	W 2%	DD 5%	W 5%	DD 5%, W 2%
Uncertainty [%]	ρ_1	10 Ohmm	0.381	0.668	0.551	0.944	0.395
	H_1	4 m	5.675	14.437	8.314	20.88	5.028
	R_1	3 m	7.616	23.452	10.882	64.03	7.194
	X_1	12.5 m	0.404	1.208	0.598	1.816	0.483
	H_2	2 m	4.24	18.999	6.346	30.831	5.314
	R_2	1.5 m	7.156	35.743	10.816	61.233	9.905
	X_2	18 m	0.163	0.526	0.244	0.761	0.202
Fitting error [%]			4.212	4.289	6.054	6.093	5.345
Rel. model distance [%]			0.588	1.768	2.548	6.882	1.391
Number of data			177	147	177	147	324

Table V. Model parameters and their uncertainties after single and simultaneous inversion of datasets with different noise and electrode array in the case of two close cylinders. *DD n*%: dipole–dipole data with *n*% of noise level; *W n*%: Wenner data with *n*% of noise level.

are sited close to each other the reliability values of the model parameters become worse (*Table V.*). On applying the simultaneous inversion method the closest estimation of the parameters can be reached in both cases.

4. Conclusions

If one processes resistivity data by means of analytical inversion the location, depth and size of the cavities along the profile can be reliably defined. The best estimation of these parameters can be achieved from data measured with a dipole–dipole array. To reduce the errors of the investigated parameters it is advisable to measure both dipole–dipole and Wenner arrays for simultaneous inversion.

Acknowledgement

This paper presents the results of an OTKA research project Nr T25370.

Appendix A

During the analytic calculations the apparent resistivity values of 2-D models are determined by applying the formulae of line sources though in practice the measurements are carried out with point sources. To investigate the model error caused by that kind of calculation the results of analytic model calculations were compared with the results of 2.5-D FD calculations using the same model and measuring parameters. The only difference between the models of the two kinds of calculation was their shape: a cylinder was used for analytic and a rectangle for FD modelling. The theory of 2.5-D calculations has been improved by PRÁCSER [1998]. The difference of the two datasets always stayed below 1% containing not only the difference of the sources but the difference in the shape of the objects as well. *Figure 7* shows an example model for such comparison. The difference between the two complete datasets (with $n = 1, \ldots,8$) was 0.987%.

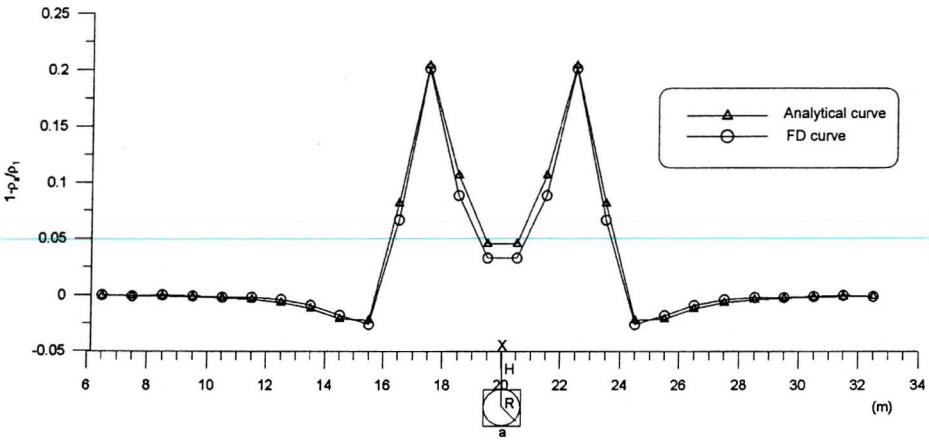

Fig. 7. Example model for investigating the error caused by using line sources instead of point sources. Electrode array: dipole–dipole, unit electrode distance: 1 m, n=5. Model parameters: ρ_2/ρ_1=100, H=1.5 m, R=0.5 m, a=1 m, X=20 m

7. ábra. Példa a pont- és vonalforrások használata miatti eltérés vizsgálatához alkalmazott modellre. Elektróda elrendezés: dipól–dipól, egységnyi elektróda távolság: 1 m, n=5. Modellparaméterek : ρ_2/ρ_1=100, H=1,5 m, R=0,5 m, a=1 m, X=20 m

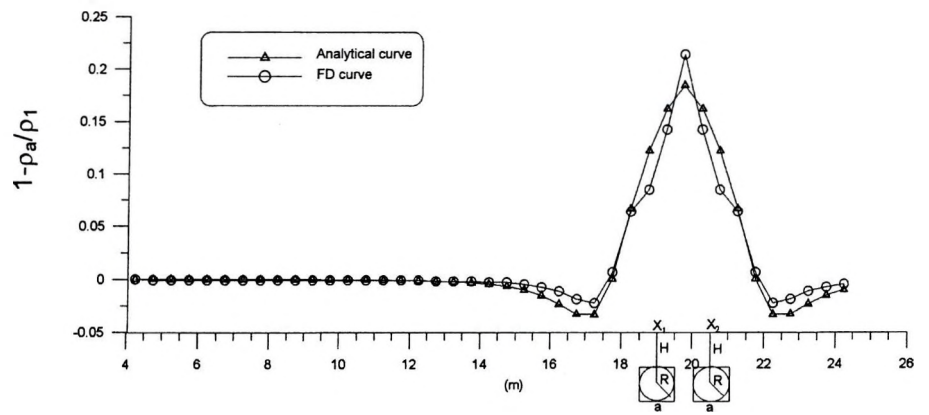

Fig. 8. Example model and theoretical curves for investigating the application of the theory of superposition in the case of two cavities. Electrode array: dipole–dipole, unit electrode distance: 0.5 m, n=5. Model parameters: ρ_2/ρ_1=100, H=1.5 m, R=0.5 m, a=1 m, X_1=19 m, X_2=20.5 m

8. ábra. Példa a szuperpozíció elve alkalmazhatóságának vizsgálatához használt két üreges modellre és elméleti görbékre. Elektróda elrendezés: dipól–dipól, egységnyi elektróda távolság: 0,5 m, n=5. Modellparaméterek: ρ_2/ρ_1=100, H=1,5 m, R=0,5 m, a=1 m, X_1=19 m, X_2=20,5 m

Appendix B

The geoelectric effect of two or more horizontal cylinders is calculated analytically by using the theory of superposition. Numeric investigations proved that this theory can be correctly used when the apparent resistivity is determined from separately calculated primary (caused by uniform halfspace) and secondary (caused by the cylinder) potentials. The control models were calculated after PRÁCSER [1998], as in App. A. In the case of cavities separated by only one distance unit from each other (*Fig. 8*) the difference of the two datasets (with n =1,...,10) was 2.54%. If one increased the distance between the objects the difference between the analytical and FD values strongly decreased.

REFERENCES

BARKER R. D. 1992: A simple algorithm for electrical imaging of the subsurface. First Break **10**, pp. 53–62

DEY A., MORRISON H. F. 1979: Resistivity modeling for arbitrarily shaped two-dimensional structures. Geophysical Prospecting **27**, pp. 106–136

DOBRÓKA M., GYULAI Á., ORMOS T., CSÓKÁS J., DRESEN L. 1991: Joint inversion of seismic and geoelectric data recorded in an underground coal mine. Geophysical Prospecting **39**, pp. 644–665

FERENCZY L. 1980: Determination of depth and dimension of near-surface cavities by means of geoelectric dipole profiling (in Hungarian). Magyar Geofizika **XXI**, 4, pp. 134–142

GYULAI Á., FERENCZY L., TAKÁCS E. 1987: Report of geophysical cavity detection having been carried out in village Emőd in connection with planning waste water canal. (in Hungarian). Report, Miskolci Egyetem Geofizikai Tanszék

GYULAI Á. 1996–97: Cavity and void detection using 1.5-D inversion methods (in Hungarian). III. report (OTKA T019088) Miskolci Egyetem Geofizikai Tanszék

GYULAI Á. 1998: Some aspects of cave research using geoelectric method (in Hungarian). Magyar Geofizika **39**, 2, pp. 43–50

LOKE M. H., BARKER R. D. 1996: Rapid least squares inversion of apparent resistivity pseudosections by a quasi-Newton method. Geophysical Prospecting **44**, pp. 131–152

LÖSCH W., MILITZER H., RÖSLER R. 1979: Zur geophysikalischen Hohlraoumortung mittels geoelektrischer Widerstandmethoden. Freiberger Forschungshefte C341, pp. 53–126

NYÁRI Zs. 1997: Examination of the possibilities of geoelectric cavity exploration using analytical modelling (in Hungarian). Magyar Geofizika **38**, 3, pp. 194–204

OWEN T. E. 1983: Detection and mapping of tunnels and caves. Development in geophysical exploration methods-5, Applied science Publishers London

SALÁT P., CSEREPES L., TARCSAI Gy., VERMES M., DRAHOS D. 1982: Statistical characteristics of information of geophysical interpretation (in Hungarian). Tankönyvkiadó Budapest

Üregkutatási célú fajlagos ellenállás mérések minőség ellenőrzött inverziója

Nyári Zsuzsanna

Üregkutatási feladatok mindennaposak a mérnökgeofizikai gyakorlatban. A fajlagos ellenállás mérésén alapuló módszereket a sokelektródás mérési rendszerek kifejlesztése óta széles körben alkalmazzák ilyen feladatok megoldására. Az új, számítógép vezérlésű adatgyűjtő rendszerek lehetővé teszik nagy mennyiségű adat rövid időn belül történő regisztrálását. A dolgozat olyan elméleti fejlesztések eredményeit ismerteti, melyek a későbbiek során alkalmazhatóvá válnak az ELGI keretében végzett felszínközeli üregkutatási feladatok megoldásában.

Az üregek lokalizálásán túl gyakran szükséges azok méretét és mélységét is megadni Kifejlesztettünk egy 2-D-s analitikus modellezésen alapuló inverziós módszert, amely az üreg helyének, mélységének és méretének számszerű értékét eredményezi, és mindezek mellett meghatározza a számított paraméterek valószínű hibáját is. A módszert sikeres numerikus tesztelése után terepi példán is alkalmaztuk.

Szimultán inverziós módszert fejlesztettünk ki annak érdekében, hogy csökkentsük az eredményül kapott modellparaméterek hibáját. Az eljárás két, különböző elektróda elrendezéssel (dipól–dipól, Wenner) mért adatrendszer együttes inverzióját végzi el. A numerikus vizsgálatok alapján kijelenthető, hogy ez az eljárás valóban megbízhatóbb paramétereket eredményez, mint a hagyományos inverzió.

ABOUT THE AUTHOR

Zsuzsanna Nyári graduated as a geophysical engineer from the University of Miskolc in 1994. She continued her post-graduation studies at the University in 1995. Then she joined the Division of Engineer Geophysics of ELGI. Topics of her main activity: electric and geoelectric field measurements and data processing in the field of engineering geophysics, development of geoelectric data processing.